

The capsids of HIV-1 and HIV-2 determine immune detection of the viral cDNA by the innate sensor cGAS in dendritic cells.

Xavier Lahaye, Takeshi Satoh, Matteo Gentili, Silvia Cerboni, Cécile Conrad, Ilse Hurbain, Ahmed El Marjou, Christine Lacabaratz, Jean-Daniel Lelièvre, Nicolas Manel

▶ **To cite this version:**

Xavier Lahaye, Takeshi Satoh, Matteo Gentili, Silvia Cerboni, Cécile Conrad, et al.. The capsids of HIV-1 and HIV-2 determine immune detection of the viral cDNA by the innate sensor cGAS in dendritic cells.. Immunity, 2013, 39 (6), pp.1132-42. 10.1016/j.immuni.2013.11.002 . inserm-00959028

HAL Id: inserm-00959028

https://inserm.hal.science/inserm-00959028

Submitted on 13 Mar 2014

HAL is a multi-disciplinary open access archive for the deposit and dissemination of scientific research documents, whether they are published or not. The documents may come from teaching and research institutions in France or abroad, or from public or private research centers.

L'archive ouverte pluridisciplinaire **HAL**, est destinée au dépôt et à la diffusion de documents scientifiques de niveau recherche, publiés ou non, émanant des établissements d'enseignement et de recherche français ou étrangers, des laboratoires publics ou privés.

*Manuscript
Click here to view linked References

Title

The HIV capsid dictates innate immune sensing of the virus by cGAS in dendritic cells

Xavier Lahaye[1,2,6], Takeshi Satoh[1,2,6], Matteo Gentili[1,2], Silvia Cerboni[1,2], Cécile Conrad[1,2], Ilse Hurbain[1,3], Ahmed El Marjou[1,3], Christine Lacabaratz[4], Jean-Daniel Lelièvre[4,5], Nicolas Manel[1,2]

[1]Institut Curie, 12 rue Lhomond, 75005 Paris, France.

[2]INSERM U932, 12 rue Lhomond, 75005 Paris, France.

[3]CNRS UMR144, 12 rue Lhomond, 75005 Paris, France

[4]INSERM U955, Université Paris Est Créteil, Faculté de Médecine, 94010 Créteil, France

[5]AP-HP, Groupe Henri-Mondor Albert-Chenevier, Immunologie clinique, 94010 Créteil, France.

[6]Equal contribution

*Correspondence: nicolas.manel@curie.fr

Summary

HIV-2 is less pathogenic than HIV-1 and may provide partial cross-protection from HIV-1-induced pathology. Although both viruses replicate in T cells of infected patients, only HIV-2 replicates efficiently in dendritic cells (DCs) and activates innate immune pathways. The mechanism of innate immune sensing, including the DC sensor, is unknown. Using mutations in the viral capsid, we dissociated sensing from productive infection in DCs. Capsid-mutated HIV-2 revealed that sensing requires viral cDNA synthesis, but not nuclear entry or genome integration. The HIV-1 capsid prevented viral cDNA sensing up to integration, allowing the virus to escape innate recognition. In contrast, DCs sensed capsid-mutated HIV-1 and enhanced stimulation of T cells in the absence of productive infection. Finally, we found that DC sensing of HIV-1 and HIV-2 required the DNA sensor cGAS. Thus, the HIV capsid dictates innate sensing of the viral cDNA by cGAS in dendritic cells. This pathway may potentially be harnessed to develop effective vaccines.

Introduction

The human immune system mounts an immune response against HIV-1, but this response is not protective in most individuals. In contrast, the related lentivirus HIV-2, which is less pathogenic than HIV-1, has been proposed to be controlled by the immune system (Rowland-Jones and Whittle, 2007). Strikingly, co-infection with HIV-1 and HIV-2 results in a better outcome than HIV-1 infection alone, including delayed progression to AIDS, suggesting that the immune response against HIV-2 induces cross-reactive protection against HIV-1 pathology (Esbjornsson et al., 2012). A key challenge is thus to understand how the immune system differs at its ability to induce immune responses against HIV-1 and HIV-2.

Dendritic cells (DCs) play a major role in the induction of immune responses. Paralleling the pathophysiological differences between the two viruses, DCs differ at their ability to induce an innate immune response against HIV-1 and HIV-2 (Manel et al., 2010; Manel and Littman, 2011). DCs do not normally get activated and efficiently infected by HIV-1 (Granelli-Piperno et al., 2004; Manel et al., 2010) while DCs are naturally infected and activated by HIV-2 (Manel et al., 2010). The absence of DC activation by HIV-1 is in part a consequence of the poor ability to infect these cells (Manel et al., 2010), which is imposed by the restriction factor SAMHD1 (Hrecka et al., 2011; Laguette et al., 2011), an Aicardi-Goutières Syndrome (AGS) susceptibility gene (Rice et al., 2009). In contrast, HIV-2 encodes the small accessory protein Vpx, which overcomes the SAMHD1 restriction in DCs. The Vpx protein is incorporated into the viral particles and released into the DCs after viral entry where it induces degradation of SAMHD1. When HIV-1 is complemented with the Vpx protein, DCs become readily infected (Goujon et al., 2006). Infected DCs in turn sense the virus and induce a concomitant innate immune response (Manel et al., 2010). In this setting, sensing of HIV-1 requires genome integration and expression of the viral capsid (Manel et al., 2010; Sunseri et al., 2011) and requires interaction between the newly synthesized viral capsid and the cellular

prolyl-isomerase Cyclophilin A (CypA) (Luban et al., 1993; Manel et al., 2010). However, whether capsid or another viral component is the actual pathogen-associated molecular pattern (PAMP) in DCs is not known. Intriguingly, DCs do not sense the reverse-transcribed HIV-1 cDNA or the incoming capsid before viral integration occurs, even in the presence of Vpx. Whether DCs are competent for sensing HIV-1 before integration occurs or whether they lack the sensing machinery remains to be determined.

Here, we focused on HIV-2 sensing by DCs to identity the mechanism of HIV-1 and HIV-2 sensing and the DC sensor.

Results

Engineering HIV-2 capsids of variable affinity for CypA to modulate sensing in DCs

In HIV-1, the interaction of capsid with CypA is required for DC activation (Manel et al., 2010). We reasoned that altering the capsid-CypA interaction might allow us to gain mechanistic insight into sensing by DCs, in particular the natural sensing of HIV-2. We noticed that two residues in HIV-1 capsid (His87-Ala88) located in the CypA-binding loop (Yoo et al., 1997), align to only one residue in HIV-2 capsid (Pro86) (**Figure 1A**), which binds less efficiently to CypA (Price et al., 2009). In HIV-1, His87-Ala88 position the Pro90, the substrate of the isomerizing activity, into the catalytic site of CypA. Strikingly, in the aligned capsid of HIV-2, the homologous Pro88 is not positioned correctly in the catalytic site of CypA (**Figures 1C, 1D**). This raised the possibility that introducing His-Ala in place of Pro86 in HIV-2 (**Figure 1B**), would positions Pro88 in the catalytic site and increase the affinity of HIV-2 capsid for CypA (HIV-2 affinity-enhanced capsid, HIVac-2), potentially perturbing innate sensing by DCs.

Expression of HIVac-2 was similar to its WT counterpart and the mutation did not alter expression of CypA in virus-producing cells (**Figure 1E**). Examination of particles by transmission electron microscopy showed a typical lentiviral ultrastructure (**data not shown**). However, HIVac-2 particles encapsidated 28 times more CypA than HIV-2 WT and 3 times more than HIV-1 (**Figure 1E and Figure S1A**). We measured the binding of recombinant capsid proteins (N-terminal domains) to recombinant CypA (**Figure S1B, S1C**). Using a co-precipitation assay, HIVac-2 capsid remained better associated to CypA compared to HIV-2 WT capsid. The association was inhibited by Cyclosporin A, an inhibitor of the capsid-CypA interaction that targets the active site of CypA. Next, microscale thermopheresis (MST) was used to estimate the dissociation constant between CypA and the capsids. The affinity of HIV-2 WT capsid to CypA was too low to be determined in this assay, while the affinity of

HIVac-2 capsid to CypA was 2.6 µM (**Figure S1D**). Thus, HIVac-2 capsid bound CypA with a higher affinity that the HIV-2 WT capsid.

DC sensing of capsid-mutated HIV-2 in the absence of productive infection

We examined the ability of HIV-2 WT and HIVac-2 to infect and activate DCs. We used a single-round HIV-2 vector that expressed GFP in DCs after integration to measure infection. Since innate sensing of HIV-1 with Vpx was independent of the viral envelope used (Manel et al., 2010), we used VSV-G-pseudotyped particles. As previously shown, HIV-2 WT was able to infect and activate DCs (**Figure 2A**) in a dose-dependent manner (**Figure 2B and Figure S2A**). Strikingly, HIVac-2 infection was completely blocked in DCs (**Figure 2A, 2B and Figure S2A**). Unexpectedly, the block did not prevent DCs sensing of HIVac-2, and HIVac-2 activated DCs more efficiently than HIV-2 WT (**Figure 2B**). Addition of Virus-Like Particles (VLPs) from the macaque simian immunodeficiency virus (SIV), a close relative of HIV-2, which provides an increased amount of Vpx and boosts abrogation of SAMHD1 restriction (Hrecka et al., 2011; Laguette et al., 2011), enhanced activation by HIVac-2 but infection was still blocked (**Figure S2A**). DC activation was characterized by production of type I interferon (**Figure 2C**) and the type I IFN response gene IP-10 (CXCL10) (**Figure 2D**) by the DCs (Manel et al., 2010). Neutralizing reagents against type I IFN effectively inhibited expression of IP-10, while CD86 expression was less dependent on type I IFN (**Figure S2B**). However, neutralizing type I IFN did not rescue the infection by HIVac-2, indicating an intrinsic effect of the mutation. Thus, mutations of the HIV-2 capsid reveal that DCs are competent for innate sensing in the absence of productive viral infection.

DC sensing of HIV-2 requires synthesis of the viral cDNA but not integration

We dissected the early steps of the viral cycle to identify the determinants of HIV-2 that are sensed in DCs (**Figure 3A**). To determine if the viral genetic material was required for sensing, we generated HIV-2 and HIVac-2 VLPs in which encapsidation of the viral genomic RNA was reduced (ΔΨ) by combining two previsouly described mutations (Griffin et al., 2001; Poeschla et al., 1998). The mutation did not prevent Gag maturation in the particles (**Figure S3A**) but reduced viral infectivity (**Figure S3B**). Despite their residual infectivity, HIV-2 and HIVac-2 VLPs with reduced RNA encapsidation were not efficient at activating DCs (**Figure S3C**). Thus, intact encapsidation of the genomic RNA in the particles is required for sensing. Next, to determine if viral DNA generated after reverse transcription was required for sensing, we generated particles lacking Vpx that are unable to abrogate the SAMHD1 restriction (ΔVpx) and are compromised for reverse transcription. HIV-2 and HIVac-2 particles lacking Vpx were not infectious and were unable to activate DCs (**Figure S3D**). To confirm that a viral cDNA was required for sensing, we added the reverse transcriptase inhibitor AZT at the time of infection. AZT prevented infection and sensing by HIV-2 (**Figures 3B, 3C**). Thus, synthesis of a viral cDNA is required for sensing. We next examined if integration was required for sensing by using Raltegravir, an inhibitor of integrase. As expected, Raltegravir blocked infection of HIV-2 WT (**Figure 3B**). However, Raltegravir did not prevent DC activation by HIV-2 WT and HIVac-2 (**Figures 3B, 3C**). To confirm that sensing occurred in the absence of integration, we inactivated the integrase (IN) by introducing a D116A mutation in its catalytic site in HIV-2 and HIVac-2 (**Figure 3A**). D116A-mutated viral particles displayed a normal profile of mature capsid protein (**Figure S3A**). HIV-2 IN D116A and HIVac-2 IN D116A maintained the ability to activate DCs (**Figures 3D, 3E**). Thus, DCs sense HIV-2 before integration and the viral cDNA is required.

DCs sense HIV-2 in the cytosol

Sensing of HIV-2 may occur in the cytosol or in the nucleus. We measured the relative abundance of the 'Late RT' HIV-2 cDNA product, the '2LTR circles' (a hallmark of nuclear entry of the viral DNA) and the 'integrated' proviral DNA after infection of DCs (**Figure 4A**). HIV-2 WT generated all forms of DNA in an AZT-sensitive manner (**Figure 4B**). HIVac-2, which activates DCs in the absence of infection, produced normal levels of Late RT viral cDNA, but no significant levels of 2LTR circles or integrated DNA (**Figure 4B, red arrows**). Treatment of HIV-2 WT with Raltegravir reduced the amount of integrated DNA and also increased the levels of 2LTR circles, but this was not the case for HIVac-2. This indicates that sensing occurs before the formation of the 2LTR circles, thus presumably in the cytosol. Next, we determined if nuclear entry was required for sensing. We mutated the central polypurine-tract (cPPT), which is required for nuclear import of the viral cDNA in dendritic cells (Riviere et al., 2010; Zennou et al., 2000) (**Figure 4A**). The mutation did not modify the Gag maturation profile of viral particles, incorporation of CypA and Vpx or efficiency of RT (**Figures S4A, S4B**). We confirmed that the cPPT mutation reduced infectivity of HIV-2 in non-dividing DCs (**Figure 4C**) and the abundance of 2LTR circles (**Figure S4B**). Sensing of cPPT-mutated HIVac-2 and HIV-2 was maintained (**Figure 4D**). Taken together, these results show that sensing requires the cDNA in the cytosol.

The HIV-1 capsid prevents cDNA sensing, escaping innate sensing up to integration

Unlike HIV-2 or HIVac-2, DCs do not sense the HIV-1 cDNA before integration (Manel et al., 2010). We hypothesized that in HIV-1 with Vpx the wild-type capsid masked the viral DNA, preventing innate sensing up to integration. To examine if the HIV-1 cDNA can stimulate an innate response, we mutated the CypA-binding loop of HIV-1 capsid to the corresponding sequence from HIVac-2 (**Figure 5A**). HIVac-1 particles incorporated more CypA (**Figures S5A, S5B**) and the HIVac-1 capsid had a higher affinity for CypA than wild-

type HIV-1 **(Figures S5C, S5D**). Similar to HIVac-2, HIVac-1 retained the ability to activate DCs and induce IP-10 in the presence of Vpx and showed a reduced infectivity (**Figures 5B, 5C, 5D**). Blockade of residual HIVac-1 integration with Raltegravir did not inhibit innate activation and IP-10 induction (**Figures 5B, 5C, 5D**). Genetic inactivation of integrase in HIVac-1 also maintained the ability to activate DCs and induce IP-10 (**Figure S5E**). Thus, the HIV-1 capsid prevents sensing of the viral cDNA, escaping innate sensing before integration, but capsid mutations lead to cDNA-dependent sensing in the cytosol similarly to HIV-2 and HIVac-2.

DCs exposed to non-integrative HIVac activate T cells

The ability of HIVac to stimulate the innate immune response induced by HIV-2 in the absence of productive infection prompted us to test if HIVac could activate T cells. First, we tested if HIVac could provide functional co-stimulatory activity (**Figure S6A**). DCs were exposed to HIVac-2 particles, leading to DC activation in the absence of infection (**Figures 6A, S6B**). In the presence of a limiting dose of an anti-CD3 antibody, added primary naïve $CD4^+$ T cells proliferated when DCs had been exposed to HIVac-2 (**Figures 6A, S6B**). This proliferation was blocked when DC activation was inhibited by AZT, and it was increased when sensing of the virus was enhanced by providing an additional dose of Vpx with VLPs. Thus, DC activation by HIVac leads to functional co-stimulation. Next, we tested if monocyte-derived DCs obtained from HIV-1-infected subjects were still competent for sensing HIVac. We super-infected the DCs with HIV-1 WT or HIVac-1 in the presence of Vpx and Raltegravir (**Figure S6C**). DCs were activated by HIVac-1, but not by the WT virus, and HIVac-1 sensing was AZT-sensitive (**Figure S6D**). Thus, DCs from HIV-1-infected subjects remain competent for innate activation by the virus. Since non-infectious HIV particles can provide antigen (Buseyne et al., 2001; Manel et al., 2010), we examined if this

would increase stimulation of autologous $CD8^+$ T cells (**Figure S6C**). DCs exposed to HIVac-1 with Vpx and Raltegravir increased the proliferation of $CD8^+$ T cells as compared to HIV-1 WT. (**Figures 6B, 6C**). This effect was blocked by AZT treatment in DCs, indicating that it required innate sensing. Thus, HIVac-1 can stimulate $CD8^+$ T cells from HIV-1-infected subjects in the absence of integration.

DC sensing of HIV-1 and HIV-2 requires cGAS

These results indicate that a cytosolic DNA sensor may be required for HIV sensing. A large number of candidate DNA sensors have been proposed in recent years in various cell types and models (Paludan and Bowie, 2013). In the transformed human cell line THP-1, the sensors cGAS, DDX41 and IFI16 were found to be required for DNA sensing leading to type I IFN production (Sun et al., 2013; Unterholzner et al., 2010; Zhang et al., 2011). We screened if these sensors could be implicated in HIV sensing by DCs derived from primary monocytes using pooled shRNA. Knock-down of DDX41 or IFI16 did not inhibit CD86 induction by HIVac-2 (**Figures S7A, S7B**). In contrast, knockdown of cGAS suppressed CD86 induction by HIVac-2. We confirmed that the shRNA inhibited by cGAS protein levels by transducing individual shRNA (**data not shown**) and selected two shRNA: shRNA #2, which modestly decreased cGAS level, and shRNA #4 which efficiently decreased cGAS level (**Figure 7A**). We stimulated shRNA-transduced DCs with HIV-1, HIV-2, HIVac-2 and the soluble RNA molecule poly(I:C) as control. cGAS knock-down prevented induction of CD86 by HIV-1, HIV-2 and HIVac-2, but not sensing of poly(I:C) (**Figure 7B**). Titrated infections confirmed that cGAS is required for induction of CD86 by HIV-1, HIV-2 and HIVac-2 (**Figure 7C**). cGAS knock-down also prevented IP-10 production after stimulation by HIV-2 and HIVac-2 (**Figure S7C**). Altogether, these data demonstrate that DC sensing of HIV-1 and HIV-2 is mediated by the DNA sensor cGAS.

Discussion

We investigated how human DCs sense HIV-1 and HIV-2. The HIV-1 capsid and its interaction with Cyclophilin A were previously found to play an essential role in innate sensing of the virus in DCs with Vpx. However, the role of capsid, the actual PAMP and the identity of its sensor were not known. By manipulating the interaction between the viral capsid and CypA through mutation (HIVac), we were able to dissociate innate sensing from productive infection of DCs. Using HIVac as an investigation tool, we report that DC sensing of HIV-2 requires reverse transcription of the viral cDNA, but not nuclear entry and integration. In contrast to HIV-2, we find that DCs cannot sense HIV-1 before integration because the viral capsid prevents cDNA sensing. Capsid-mutated HIV-1 revealed that DCs are nonetheless competent for HIV-1 sensing of the viral cDNA before integration. Such capsid-mutated particles elicit innate immunity in DCs and activate T cells in the absence of viral replication. Finally, we demonstrate that human DCs use the DNA sensor cGAS to sense the viral cDNA. Thus, our results establish that, in DCs, the cytosolic viral cDNA is an HIV PAMP and that the viral capsid dictates whether this cDNA will escape sensing or will be sensed through cGAS.

Various candidate DNA sensors have been proposed in the recent years (Paludan and Bowie, 2013) that seem to operate differently between human and mouse, between cell types and between DNA stimuli (Abe et al., 2013; Brunette et al., 2012; Cavlar et al., 2013; Sun et al., 2013; Unterholzner et al., 2010; Zhang et al., 2011) and this complexity, that may reflect functional redundancy, has not been resolved. In human myeloid dendritic cells, the sensor(s) that are required for sensing cytosolic DNA are not yet known. One of the DNA sensors, cGAS, synthetizes cyclic GMP-AMP (cGAMP) upon DNA sensing. cGAMP was recently detected in DCs infected by HIV-1 in the presence of Vpx (Gao et al., 2013), but whether

cGAS or any other DNA sensor is actually required for innate sensing in DCs was not evaluated. Using RNAi, we demonstrate that cGAS is essential (non-redundant) for DC sensing of HIV.

The demonstration that the wild-type HIV-1 capsid effectively prevents sensing of the viral cDNA up to integration provides an explanation for the absence of innate immune response up to viral integration in DCs (even in the presence of Vpx) and to the ability of HIV-1-derived lentiviral vectors to transduce DCs in the absence of innate sensing against the lentivector itself (Manel et al., 2010; Satoh and Manel, 2013). Later in the viral cycle, after integration and productive infection, DC can sense HIV-1 and this was shown to require expression of newly synthesized capsid (Manel et al., 2010; Sunseri et al., 2011). We proposed that sensing in this setting implicated unmasking of remaining unintegrated cDNA products through interaction with CypA (Manel and Littman, 2011). The demonstration that the DNA sensor cGAS is required for HIV-1 sensing argues in favor of this model (**Figure S8**).

How does the HIV-1 capsid prevent sensing of the viral cDNA up to integration? By increasing the capsid affinity for CypA through mutations, we find that the cDNA gets sensed in the absence of integration (**Figure S8**). This suggests that the HIV-1 capsid has evolved an optimal interaction with CypA that allows cell infection while masking innate sensing of the cDNA up to integration (**Figure S8**). In contrast, wild-type HIV-2 simultaneously infects the DCs and triggers innate sensing of its cDNA before integration (**Figure S8**). This suggests that the HIV-2 capsid accommodates a flexible conformation that can both unmask the cDNA in the cytosol leading to sensing and also mediate infection. HIV-2 seems to achieve this flexibility through a minimal interaction of its capsid with CypA. Nonetheless, HIV-2 is

amenable to increased affinity for CypA through mutation (HIVac-2 capsid), leading to sensing in the absence of infection, like HIVac-1. The natural balance between infection and innate sensing in HIV-2 may contribute to the reduced pathogenicity of this virus, while the ability of HIV-1 to prevent sensing of its cDNA may contribute to its immune escape.

Three evidences indicate that the sensing is cytosolic. First, 2LTR circles, a hallmark of nuclear import, are not significantly detected when DCs respond to HIVac-2. Second, the cPPT is not required for innate sensing. Even though the role of the cPPT in nuclear import is incompletely understood (Dvorin et al., 2002; Riviere et al., 2010; Zennou et al., 2000), we confirmed that in the experimental conditions that we used, disruption of the cPPT reduces the abundance 2LTR circles but did not modify the abundance Late RT cDNA, indicative of inhibition before or at nuclear import. Finally, we find that cGAS, a cytosolic DNA sensor (Sun et al., 2013), is essential for sensing.

DC sensing of HIV cDNA also requires Vpx, which abrogates the SAMHD1 restriction. SAMHD1 was previously identified as an AGS-susceptibility gene, a syndrome characterized by apparent uncontrolled induction of a type I interferon innate response. SAMHD1 was also found to hydrolyze dNTP in cells, and it is thought that SAMHD1 removal increases retroviral cDNA levels by replenishment of the dNTP pool (Lahouassa et al., 2012). Our results establish the first direct link between the negative regulation of retroviral DNA synthesis by SAMHD1 and induction of an innate immune induced by this DNA. Interestingly, innate sensing of HIV-1 DNA was reported in cells deficient for TREX1 (Yan et al., 2010), another AGS-related gene (Rice et al., 2007). In contrast to sensing in intact human DCs, DNA sensing in TREX1-deficient cells occurs in the context of the wild-type HIV-1 capsid. Furthermore, TREX1 is a proviral factor (Yan et al., 2009) while SAMHD1 is

a restriction factor (Hrecka et al., 2011; Laguette et al., 2011). Overall, while sensing in DCs and in TREX1-deficient cells converge on DNA sensing regulated by AGS genes, the viral determinants implicated appear to be distinct.

While pathogenesis induced by HIV-1 and HIV-2 is associated with chronic and non-specific general immune activation, the virus-specific immune response induced against HIV-2 correlates with its reduced pathogenicity (Rowland-Jones and Whittle, 2007) and likely contributes its anti-pathogenic activity on HIV-1 (Esbjornsson et al., 2012). Furthermore, immunization of macaques with a live-attenuated strain of HIV-2 (Putkonen et al., 1995) protects against infection with a pathogenic SIVmac strain. This indicates that HIV-2 contains inducers of anti-HIV/SIV immunity, which have not been successfully matched in humans by non-lentiviral vaccine candidates. Given the central role of dendritic cells in coupling innate sensing to induction of adaptive immunity, cytosolic sensing of the HIV-2 cDNA through cGAS in DCs likely shapes these anti-HIV-2 immune responses. We find that a similar DC sensing can be obtained in the absence of productive infection of the DCs. Capsid-mutated HIVac-2 and HIVac-1 can autonomously activate DCs (with Vpx) in the absence of viral integration, hence satisfying the definition of a DC adjuvant, and lead to functional co-stimulation of naïve $CD4^+$ T cells and stimulation of primary $CD8^+$ T cells from HIV-1-infected subjects, respectively. These effects on T cells were blocked by inhibition of reverse-transcription in DCs, demonstrating that innate sensing of the viral cDNA in DCs was required. While antigen specificity of the proliferating cells was not examined, previous work showed that DCs exposed to non-infectious particles comparable to HIVac-1 induce antigen-specific response of $CD8^+$ T cells (Buseyne et al., 2001; Manel et al., 2010). It will be important to determine the immunogenicity of HIVac-1 in relevant animal models, with or without additional antigens. Though no adjuvant is effective to date for HIV-1 vaccination,

the pathway we described provides several putative advantages. First, HIV-2 is known to induce protection against HIV-1 pathogenesis, unlike current adjuvants. Second, the response is specific to HIV, unlike generic adjuvants such poly(I:C). Finally, beyond capsid-mutated viruses, our results suggest that DC-targeted agonists of the cGAS pathway in the presence of antigen may recapitulate this response. Our results hence provide a molecular basis for manipulating this response in order to control or reduce pathogenesis in HIV-1 infected patients and to induce anti-HIV-1 immunity.

Altogether, we have identified a mechanism of HIV-1 and HIV-2 sensing in DCs, which is tightly regulated by the affinity of capsid for CypA and which requires the DNA sensor cGAS. Viral capsid mutations can attenuate the virus and favor triggering of this innate response. Stimulation of this response in DCs will likely contribute to generating a more effective immune response against the virus.

Experimental Procedures

Constructs

The HIV-1 WT construct was NL4-3 ΔvifΔvprΔvpuΔenvΔnef encoding GFP in nef and the HIV-2 WT construct was ROD9 ΔenfΔnef encoding GFP in nef as previously described (Manel et al., 2010). HIV-1 IN D116A was previously described (Manel et al., 2010). Mutants HIV-1 V86I-IAP91LPA-M96L (HIVac-1) and HIV-2 P86HA (HIVac-2), IN D116A, ΔΨ, ΔVpx, ΔcPPT were generated by overlapping PCR mutagenesis. Combinatory mutations were generated by standard molecular biology procedures. In the HIVac-1 D116A experiment, a NL4-3 backbone restored for the SL9 class I epitope was used. Corresponding mutagenized sequences are listed in **Table S1**. HIV-2 ΔΨ was generated by combining two previously described packaging signal deletions (Griffin et al., 2001; Poeschla et al., 1998). CMV-VSVG, psPAX2, LKO1puro and pSIV3+ were described elsewhere (Manel et al., 2010). shRNA against IFI16, DDX41 and cGAS (gene MB21D1) were in the LKO.1-puro vector (SIGMA) and are listed in **Table S2**. Human CypA was amplified from cDNA generated by reverse transcription of total RNA extracted from PBMCs. In all final constructs, the entire DNA fragments originating from the PCR and encompassing the restriction sites used for cloning were fully verified by sequencing. Full length human CypA and the NTD of HIV-1 (P_1IVQ...TSIL$_{151}$), HIV-2 WT (P_1VQH...TNIL$_{150}$) and HIVac-2 (P_1VQH...TNIL$_{151}$) capsids were amplified by PCR and cloned in a pDONOR vector (Invitrogen) using the BP Gateway reaction. A TEV cleavage site (DIPTTENLYFQG) was added to the N-terminus of each protein. CypA was transferred using the LR Gateway reaction into pDEST-His-GST and pDEST-His (pDEST17) and the capsid NTDs were transferred using the LR Gateway reaction into pDEST-His-ZZ (Braud et al., 2005). Plasmid DNA was purified using with the low endotoxin HiPure plasmid kit (Invitrogen).

Recombinant plasmid DNA did not induce dendritic cell maturation, and viral-producing cells were washed after DNA transfection.

Cells.

GHOST (GHOST X4R5), 293FT and HL116 cells were cultured in DMEM, 10% fetal bovine serum (FBS) (Gibco), Penicillin-Streptomycin (Gibco). HL116 cells were supplemented with 2% HAT (Invitrogen). Peripheral blood mononuclear cells were isolated from buffy coats from normal human donors using Ficoll-Paque PLUS (GE). Human $CD14^+$ cells were isolated by a positive selection with anti-human CD14 magnetic beads (Miltenyi). Purity was checked by flow cytometry using an anti-CD14 antibody (antibodies are listed in **Table S3**) and purity was superior to 99%. $CD14^+$ and T cells were cultured in RPMI medium, 10% FBS (Biowest), Penicillin-Streptomicin, Gentamicin (50 µg/ml, Gibco) and HEPES (Gibco) in the presence of recombinant human GM-CSF (Miltenyi) at 10 ng/ml and IL-4 (Miltenyi) at 50 ng/ml. Fresh media was added at day 3, and cells were stimulated or infected at day 4. Human naïve $CD4^+$ T cells were sorted by positive selection with anti-human CD4 magnetic beads (Miltenyi) followed by sorting on a BD FACSAria IIIu as $CD4^+CD8ß^-CD27^+CD45RO^-$.

Virus production.

Viral particles were produced by transfection of 293FT cells in 6-well plates with 3 µg DNA and 8 µl TransIT-293 (Mirus Bio) per well; for VSV-G pseudotyped SIVmac VLPs, 0.4 µg CMV-VSVG and 2.6 µg $pSIV3^+$; for HIV-1 or HIV-2 VSV-G pseudotyped viruses, 0.4 µg CMV-VSVG and 2.6 µg HIV DNA; for shRNA vectors, 0.4 µg CMV-VSV-G, 1 µg psPAX2 and 1.6 µg LKO1puro-derived shRNA or pTRIP vector. One day after transfection, media was removed, cells were washed out once and fresh media was added. Viral supernatants were harvested one day later, filtered at 0.45 µM, aliquoted and frozen at -80°C. Viral titers

were measured on GHOST cell titration as previously described (Manel et al., 2010). RT activity in viral supernatants was measured using either a colorimetric kit containing HIV-1 RT as a standard (Roche) or using the SG-PERT assay (Pizzato et al., 2009) using M-MuLV RT (Finnzyme) as a standard (1 pg/ml of HIV-1 RT standard corresponds to 185 µU/ml in the SG-PERT assay). Viral supernatants did not induce dendritic cell activation in the absence infection.

Infections.

At day 4 of MDDC differentiation, cells were harvested, counted and resuspended in fresh media at a concentration of one million per ml with 5 µg/ml polybrene, GM-CSF and IL-4, and 100 µl was aliquoted in round-bottomed 96-well plates. For infection, 50 µl of media or SIVmac VLPs were first added. One-hundred microlitres of media or dilutions of viral supernatants. Azidothymidine (AZT, SIGMA) or Raltegravir (RAL, Euromedex) were added respectively at 24 µM and 20 µM. For type I IFN neutralization, a cocktail containing 6 µg/ml recombinant B18R (eBioscience), 1.2 µg/ml monoclonal anti-IFNα (eBioscience), 1.2 µg/ml monoclonal anti-IFNß (eBioscience), 1.2 µg/ml monoclonal anti-IFNß (Millipore) and 0.6 µg/ml monoclonal anti-IFNAR2 (Millipore) were added. 48 hours after infection, cell culture supernatants were harvested and ultraviolet-irradiated to inactivate free virus. Supernatants were subsequently used for a quantitative bioassay for IFNs or IP-10 quantification. Cell-surface staining of CD86 (eBioscience) was also performed 48 h after exposure and analyzed on a BD Accuri C6 or a BD FACSVerse flow cytometer. Stimulation and DCs activation were positively controlled by treatment with high molecular weight poly(I:C) (Invivogen).

Sensors knock-down

For screening of the sensors, fresh monocytes were co-transduced with a control empty vector

LKO.1-puro or a pool of five shRNA vectors in LKO.1-puro against IFI16, DDX41 or cGAS (SIGMA) as previously described (Manel et al., 2010; Satoh and Manel, 2013). Knock-down efficiency was measured by quantitative PCR on day 4 samples. For validation experiments, fresh monocytes were transduced with an empty vector, a shRNA vector targeting LacZ or individual shRNA vectors targeting cGAS. Puromycin was added at day 2 (2 ng/ml). At day 4, DCs were harvested, counted, seeded at 0.5 million per ml in 96-well U bottom plate as described above and infected or stimulated in 200 µl of final volume. Surface CD86 expression and soluble IP-10 production were measured at day 6. Knock-down efficiency was measured by quantitative PCR at day 4 and/or western blotting at day 6. For CD86 expression, donors for which the background of CD86 expression was higher than 20% in control samples, or for which the highest dose of stimulation of control shRNA samples did not show an induction of at least 20% of CD86-positive cells were excluded from the analysis.

Quantitative bioassay for IFNs.

Supernatants were assayed for IFN activity using the HL116 cell line, which carries a luciferase reporter controlled by the IFN-inducible 6-16 promoter, as previously described (Uze et al., 1994). In brief, the reporter cells were exposed to cell culture supernatants for 5 h and assayed for luciferase activities (Promega), which were then translated to IFN activities by using a standard curve generated from a serial dilution of human IFNalpha-2a (ImmunoTools).

IP-10 protein quantification

IP-10 concentration was measured on pure or 10-fold dilutions (controls and HIV infection) or 100-fold dilutions (poly(I:C)) of supernatants from infected DCs. IP-10 concentration was

measured using a Human IP-10 cytometric assay (BD) according to manufacturer's protocol. Data was acquired on a BD FACSVerse (BD) and analyzed in FCAP Array (BD).

HIV-2 Real-time PCR.

Total cellular DNA was harvested using a Nucleospin Tissue kit (Machery-Nagel). Real-time PCR analysis was adapted from (Brussel and Sonigo, 2003) and performed in a Roche LightCycler 480 using Roche 480 SYBR Green I master reagent in 20 µl final volume per well according to manufacturer specifications. Each sample was measured in triplicate for all primers. For beta-globin, primers were bglobin-f CCCTTGGACCCAGAGGTTCT (SEQ ID No:43) and bglobin-r CGAGCACTTTCTTGCCATGA (SEQ ID No:44). For Late RT, primers were hiv2-3'U3-fwd GAAGGGATGTTTTACCATTTAGTTA (SEQ ID No:45) and hiv2-psi-rev GTTCCAAGACTTCTCAGTCTTCTTC (SEQ ID NO:46). For 2LTR, primers were hiv2-3'U3-rev TAACTAAATGGTAAAACATCCCTTC (SEQ ID NO:47) and hiv2-R-fwd GTTCTCTCCAGCACTAGCAGGTA (SEQ ID NO:48). For integrated DNA two rounds of amplification were performed. For the first round, primers were alu1 GCCTCCCAAAGTGCTGGGATTACAG (SEQ ID NO:49) and hiv2-r AAGGGTCCTAACAGACCAGGGTCT (SEQ ID NO:50). For the second round, 1 µl of first-round reaction was used as template, and primers were hiv2-f2 GCAGGTAGAGCCTGGGTGTTC (SEQ ID NO:51) and hiv2-r2 CAGGCGGCGACTAGGAGAGAT (SEQ ID NO:52). Cycling conditions were 1x 95°C 5'; 35x 95°C 10"-50°C 20"-72°C 30". Relative concentrations of Late RT, 2LTR and integrated viral DNA were calculated relative to beta-globin using the ΔCt method.

Naïve T cell proliferation assay

Sorted resting naïve $CD4^+$ T cells were stained with a Cell Proliferation Dye (CPD670, eBioscience). $2x10^4$ resting T cells were co-cultured with $4x10^3$ autologous infected DCs without cytokines in 96-well U bottom plates. Ten-fold dilutions of anti-CD3 antibody (from 10 pg/ml to 100 ng/ml) or no antibody were added to replicate wells. At day 4 and day 5 post-stimulation, an aliquot of the cells was fixed and analyzed by flow cytometry on a BD FACSVerse. The optimal costimulation-dependent concentrations of anti-CD3 were 100 or 10 pg/ml depending of the donor.

Stimulation of $CD8^+$ T cells from HIV-1-infected individuals

Blood samples were collected from HIV-1-positive subjects followed in the department of clinical immunology of Henri Mondor Hospital, Créteil, France (**Table S4**). Approval and written informed consent from all subjects were obtained before study initiation. The study was approved by the ethical committee CCP IX Ile de France, Henri Mondor Hospital, Créteil, France. Fresh peripheral blood mononuclear cells were isolated from blood patients. Monocytes were isolated by a positive selection with anti-human CD14 magnetic beads (Miltenyi) and differentiated in DCs for 3 days. The CD14-negative fraction was cultured in RPMI medium, 10% FBS (Biowest), Penicillin-Streptomicin, Gentamicin (50 µg/ml, Gibco) and HEPES (Gibco) in the presence recombinant human IL-2 at 50 U/ml and 25 µM AZT or in X-VIVO 20 (LONZA), Penicillin-Streptomicin in the presence recombinant human IL-2 at 50 U/ml, 10 ng/ml recombinant human IL-7 (Miltenyi) and 25 µM AZT. At day 3, DCs were super-infected with VSV-G-pseudotyped HIV-1 or HIVac-1 in the presence of SIVmac VLPs, 20 µM Raltegravir and 25 µM AZT. At day 4, autologous total $CD8^+$ T cells were isolated from the CD14-negative fraction in culture by a positive selection with anti-human CD8 magnetic beads (Miltenyi). Sorted $CD8^+$ T cells were stained with a Cell Proliferation Dye (CPD670, eBioscience). $5x10^4$ DCs were infected and co-cultured one day after with 10^5

$CD8^+$ T cells in 250 µl in 96-well round bottom plates. In some wells, Staphylococcal Enterotoxin B was added at 1 µg/ml (Toxin Technology). At day 5 of DC differentiation (day 1 of co-culture), CD86 and GFP expression was analyzed in DCs from replicate wells in the absence of T cells. At day 2 of co-culture, IL-2 was added in at 20 U/ml and at day 5 of coculture, a half of the coculture was processed for staining and the other half was kept in fresh medium with IL-2 at 20 U/ml for 2 more days and processed for staining at day 7 of co-culture. Cells were stained with a viability dye (LIVE/DEAD Aqua, Invitrogen) and with anti-CD8-PE-Cy5.5 and anti-CD4-eFluor-450. Cells were fixed and analyzed on BD FACSVerse.

Acknowledgements

The authors declare no conflict of interest. NM, TS and XL designed the study. XL and TS performed most of the experiments. NM, SC and MG performed some experiments. NM, TS and XL wrote the article and prepared figures. CC provided technical help. IH and AEM provided platform help. CL and JDL contributed to experiments with samples from HIV-1-infected patients. We are grateful to Sandra Pellegrini for the gift of the HL116 cell line. We thank Dan Littman, Philippe Benaroch and Ana-Maria Lennon for critical reading of the manuscript and Sebastian Amigorena for comments. We thank Olivier Lantz for helpful discussions. We thank Mathieu Maurin, Carolina Martinez, Maxime Touzot, Maximilien Grandclaudon, Isabelle Peguillet, François-Xavier Gobert, Laurent Zablocki, Mohamed El Amine Mechalikh, the Institut Pasteur Macromolecules Biophysics and Interactions platform and the Houdusse lab for technical assistance. We thank the PICT-IBiSA electron microscopy facility, the Cytometry facility, the Proteins and Antibody facility and the BSL3 facility of Institut Curie. This work was supported by Institut Curie, Institut National de la Santé et de la Recherche Médicale (INSERM), ATIP-Avenir program, Agence Nationale de Recherche sur le SIDA (ANRS), Ville de Paris Emergence program, European FP7 Marie Curie Actions, European Research Council, LABEX VRI and LABEX DCBIOL.

References

Abe, T., Harashima, A., Xia, T., Konno, H., Konno, K., Morales, A., Ahn, J., Gutman, D., and Barber, G.N. (2013). STING Recognition of Cytoplasmic DNA Instigates Cellular Defense. Mol Cell *50*, 5-15.

Braud, S., Moutiez, M., Belin, P., Abello, N., Drevet, P., Zinn-Justin, S., Courcon, M., Masson, C., Dassa, J., Charbonnier, J.B., *et al.* (2005). Dual expression system suitable for high-throughput fluorescence-based screening and production of soluble proteins. J Proteome Res *4*, 2137-2147.

Brunette, R.L., Young, J.M., Whitley, D.G., Brodsky, I.E., Malik, H.S., and Stetson, D.B. (2012). Extensive evolutionary and functional diversity among mammalian AIM2-like receptors. J Exp Med *209*, 1969-1983.

Brussel, A., and Sonigo, P. (2003). Analysis of early human immunodeficiency virus type 1 DNA synthesis by use of a new sensitive assay for quantifying integrated provirus. Journal of virology *77*, 10119-10124.

Buseyne, F., Le Gall, S., Boccaccio, C., Abastado, J.P., Lifson, J.D., Arthur, L.O., Riviere, Y., Heard, J.M., and Schwartz, O. (2001). MHC-I-restricted presentation of HIV-1 virion antigens without viral replication. Nat Med *7*, 344-349.

Cavlar, T., Deimling, T., Ablasser, A., Hopfner, K.P., and Hornung, V. (2013). Species-specific detection of the antiviral small-molecule compound CMA by STING. EMBO J.

Dvorin, J.D., Bell, P., Maul, G.G., Yamashita, M., Emerman, M., and Malim, M.H. (2002). Reassessment of the roles of integrase and the central DNA flap in human immunodeficiency virus type 1 nuclear import. Journal of virology *76*, 12087-12096.

Esbjornsson, J., Mansson, F., Kvist, A., Isberg, P.E., Nowroozalizadeh, S., Biague, A.J., da Silva, Z.J., Jansson, M., Fenyo, E.M., Norrgren, H., and Medstrand, P. (2012). Inhibition of HIV-1 disease progression by contemporaneous HIV-2 infection. N Engl J Med *367*, 224-232.

Gao, D., Wu, J., Wu, Y.T., Du, F., Aroh, C., Yan, N., Sun, L., and Chen, Z.J. (2013). Cyclic GMP-AMP synthase is an innate immune sensor of HIV and other retroviruses. Science *341*, 903-906.

Goujon, C., Jarrosson-Wuilleme, L., Bernaud, J., Rigal, D., Darlix, J.L., and Cimarelli, A. (2006). With a little help from a friend: increasing HIV transduction of monocyte-derived dendritic cells with virion-like particles of SIV(MAC). Gene Ther *13*, 991-994.

Granelli-Piperno, A., Golebiowska, A., Trumpfheller, C., Siegal, F.P., and Steinman, R.M. (2004). HIV-1-infected monocyte-derived dendritic cells do not undergo maturation but can elicit IL-10 production and T cell regulation. Proc Natl Acad Sci U S A *101*, 7669-7674.

Griffin, S.D., Allen, J.F., and Lever, A.M. (2001). The major human immunodeficiency virus type 2 (HIV-2) packaging signal is present on all HIV-2 RNA species: cotranslational RNA encapsidation and limitation of Gag protein confer specificity. Journal of virology *75*, 12058-12069.

Hrecka, K., Hao, C., Gierszewska, M., Swanson, S.K., Kesik-Brodacka, M., Srivastava, S., Florens, L., Washburn, M.P., and Skowronski, J. (2011). Vpx relieves inhibition of HIV-1 infection of macrophages mediated by the SAMHD1 protein. Nature *474*, 658-661.

Laguette, N., Sobhian, B., Casartelli, N., Ringeard, M., Chable-Bessia, C., Segeral, E., Yatim, A., Emiliani, S., Schwartz, O., and Benkirane, M. (2011). SAMHD1 is the dendritic- and myeloid-cell-specific HIV-1 restriction factor counteracted by Vpx. Nature *474*, 654-657.

Lahouassa, H., Daddacha, W., Hofmann, H., Ayinde, D., Logue, E.C., Dragin, L., Bloch, N., Maudet, C., Bertrand, M., Gramberg, T., *et al.* (2012). SAMHD1 restricts the replication of human immunodeficiency virus type 1 by depleting the intracellular pool of deoxynucleoside triphosphates. Nat Immunol *13*, 223-228.

Luban, J., Bossolt, K.L., Franke, E.K., Kalpana, G.V., and Goff, S.P. (1993). Human immunodeficiency virus type 1 Gag protein binds to cyclophilins A and B. Cell *73*, 1067-1078.

Manel, N., Hogstad, B., Wang, Y., Levy, D.E., Unutmaz, D., and Littman, D.R. (2010). A cryptic sensor for HIV-1 activates antiviral innate immunity in dendritic cells. Nature *467*, 214-217.

Manel, N., and Littman, D.R. (2011). Hiding in plain sight: how HIV evades innate immune responses. Cell *147*, 271-274.

Paludan, S.R., and Bowie, A.G. (2013). Immune Sensing of DNA. Immunity *38*, 870-880.

Pizzato, M., Erlwein, O., Bonsall, D., Kaye, S., Muir, D., and McClure, M.O. (2009). A one-step SYBR Green I-based product-enhanced reverse transcriptase assay for the quantitation of retroviruses in cell culture supernatants. J Virol Methods *156*, 1-7.

Poeschla, E., Gilbert, J., Li, X., Huang, S., Ho, A., and Wong-Staal, F. (1998). Identification of a human immunodeficiency virus type 2 (HIV-2) encapsidation determinant and transduction of nondividing human cells by HIV-2-based lentivirus vectors. Journal of virology *72*, 6527-6536.

Price, A.J., Marzetta, F., Lammers, M., Ylinen, L.M., Schaller, T., Wilson, S.J., Towers, G.J., and James, L.C. (2009). Active site remodeling switches HIV specificity of antiretroviral TRIMCyp. Nat Struct Mol Biol *16*, 1036-1042.

Putkonen, P., Walther, L., Zhang, Y.J., Li, S.L., Nilsson, C., Albert, J., Biberfeld, P., Thorstensson, R., and Biberfeld, G. (1995). Long-term protection against SIV-induced disease in macaques vaccinated with a live attenuated HIV-2 vaccine. Nat Med *1*, 914-918.

Rice, G., Newman, W.G., Dean, J., Patrick, T., Parmar, R., Flintoff, K., Robins, P., Harvey, S., Hollis, T., O'Hara, A., *et al.* (2007). Heterozygous mutations in TREX1 cause familial chilblain lupus and dominant Aicardi-Goutieres syndrome. Am J Hum Genet *80*, 811-815.

Rice, G.I., Bond, J., Asipu, A., Brunette, R.L., Manfield, I.W., Carr, I.M., Fuller, J.C., Jackson, R.M., Lamb, T., Briggs, T.A., *et al.* (2009). Mutations involved in Aicardi-Goutieres syndrome implicate SAMHD1 as regulator of the innate immune response. Nat Genet *41*, 829-832.

Riviere, L., Darlix, J.L., and Cimarelli, A. (2010). Analysis of the viral elements required in the nuclear import of HIV-1 DNA. Journal of virology *84*, 729-739.

Rowland-Jones, S.L., and Whittle, H.C. (2007). Out of Africa: what can we learn from HIV-2 about protective immunity to HIV-1? Nat Immunol *8*, 329-331.

Satoh, T., and Manel, N. (2013). Gene transduction in human monocyte-derived dendritic cells using lentiviral vectors. Methods Mol Biol *960*, 401-409.

Sun, L., Wu, J., Du, F., Chen, X., and Chen, Z.J. (2013). Cyclic GMP-AMP synthase is a cytosolic DNA sensor that activates the type I interferon pathway. Science *339*, 786-791.

Sunseri, N., O'Brien, M., Bhardwaj, N., and Landau, N.R. (2011). Human immunodeficiency virus type 1 modified to package Simian immunodeficiency virus Vpx efficiently infects macrophages and dendritic cells. Journal of virology *85*, 6263-6274.

Unterholzner, L., Keating, S.E., Baran, M., Horan, K.A., Jensen, S.B., Sharma, S., Sirois, C.M., Jin, T., Latz, E., Xiao, T.S., *et al.* (2010). IFI16 is an innate immune sensor for intracellular DNA. Nat Immunol *11*, 997-1004.

Uze, G., Di Marco, S., Mouchel-Vielh, E., Monneron, D., Bandu, M.T., Horisberger, M.A., Dorques, A., Lutfalla, G., and Mogensen, K.E. (1994). Domains of interaction between alpha interferon and its receptor components. J Mol Biol *243*, 245-257.

Yan, N., Cherepanov, P., Daigle, J.E., Engelman, A., and Lieberman, J. (2009). The SET complex acts as a barrier to autointegration of HIV-1. PLoS Pathog *5*, e1000327.

Yan, N., Regalado-Magdos, A.D., Stiggelbout, B., Lee-Kirsch, M.A., and Lieberman, J. (2010). The cytosolic exonuclease TREX1 inhibits the innate immune response to human immunodeficiency virus type 1. Nat Immunol *11*, 1005-1013.

Yoo, S., Myszka, D.G., Yeh, C., McMurray, M., Hill, C.P., and Sundquist, W.I. (1997). Molecular recognition in the HIV-1 capsid/cyclophilin A complex. J Mol Biol *269*, 780-795.

Zennou, V., Petit, C., Guetard, D., Nerhbass, U., Montagnier, L., and Charneau, P. (2000). HIV-1 genome nuclear import is mediated by a central DNA flap. Cell *101*, 173-185.

Zhang, Z., Yuan, B., Bao, M., Lu, N., Kim, T., and Liu, Y.J. (2011). The helicase DDX41 senses intracellular DNA mediated by the adaptor STING in dendritic cells. Nat Immunol *12*, 959-965.

Figure Legends

Figure 1 Modulation of HIV-2 capsid affinity for Cyclophilin A, a host factor implicated in innate sensing by dendritic cells

(A) Alignment of the CypA-binding loops of HIV-1 and HIV-2 capsids. H87A88 and P90 in HIV-1, and P86 and P88 in HIV-2 are indicated in bold.

(B) Sequence of the putative HIV-2 affine capsid, HIVac-2 (HIV-2 P86HA mutation), same region as in (A).

(C) The structure of the HIV-2 capsid N-terminal domain (red, PDB 2WLV) is aligned on the HIV-1 capsid NTD bound to CypA (respectively blue and gray, PDB 1AK4).

(D) Magnification of the CypA catalytic site bound to HIV-1 (respectively gray and blue, PDB 1AK4) or HIV-2 capsids (red, PDB 2WLV). The two residues H87A88 in HIV-1 capsid position the proline substrate to interact with H125 and R55 in CypA. In HIV-2, P86 induces a distortion in the loop that prevents these interactions.

(E) The P86HA mutation in HIVac-2 leads to CypA incorporation in viral particles. Left, protein expression in virus-producing cells. HIV-1, HIV-2 or HIVac-2 viral proteins were analyzed by western blotting against Gag/Capsid, CypA and actin. Right, viral particles were analyzed by western blotting against Gag/Capsid and CypA.

Figure 2 Dendritic cells sense HIVac-2 in the absence of infection.

(A) GFP and CD86 expression in MDDCs 48 hours after infection with HIV-2 WT or HIVac-2 encoding GFP in Nef and pseudotyped with VSV-G in the presence of SIVmac VLPs.

(B) Dose-response expression of GFP and CD86 as in (A) (n=7).

(C) Type I IFN production by MDDCs infected with VSV-G pseudotyped HIV-2 WT or HIVac-2, or treated with poly(I:C) (pIC) for 48 hours. (n=7).

(D) IP-10 production (n=4; paired t-test on log-transformed data) by MDDCs infected with VSV-G pseudotyped HIV-2 WT or HIVac-2 in the presence of SIVmac VLPs, or treated with poly(I:C) (pIC) for 48 hours. Dilution factors of the input viral inoculum are indicated.

Figure 3 Dendritic cells sensing of HIV-2 requires a viral cDNA but integration is dispensable.

(A) Principles of the experiments. Left, mutations introduced in HIV-2. Right, early steps of the HIV replication cycle affected by the mutation (ΔΨ, ΔVpx, IN D116A) or the drugs (AZT, RAL).

(B) GFP and CD86 expression in MDDCs infected with HIV-2 WT or HIVac-2 in the absence of presence of AZT or RAL and in the presence of SIVmac VLPs.

(C) Dose-response expression of CD86 as in (B) (n=4).

(D) GFP and CD86 expression in MDDCs infected with HIV-2 WT or HIVac-2 with or without a mutation in the catalytic site of integrase (IN D116A) in the presence of SIVmac VLPs.

(E) Dose-response expression of CD86 as in (D) (n=6).

Figure 4 Dendritic cells sense HIV-2 viral cDNA in the cytosol.

(A) Principles of the experiments. Left, mutations introduced in HIV-2. Right, the viral DNA species detected by the assay (Late RT, 2LTR circles and Integrated) and the steps inhibited by the drugs (AZT, RAL) and the mutation (ΔcPPT).

(B) Quantification of Late RT, 2LTR circles and integrated viral cDNA products 24 hours after infection of DCs with HIV-2 WT or HIVac-2 in the presence of SIVmac VLPs. Cells were treated with AZT or Raltegravir (RAL) (n=3; representative data for 1 donor is shown).

Red arrows indicate the absence of 2LTR-circles and integrated DNA after infection by HIVac-2.

(C) GFP and **(D)** CD86 expression in DCs infected with HIV-2 or HIVac-2 that is wild-type or mutated cPPT, in the presence of SIVmac VLPs (n=4).

Figure 5 Dendritic cells are competent for sensing of HIV-1 in the absence of infection but the wild-type viral capsid prevents innate sensing of the cDNA up to integration.

(A) Alignment of the CypA-binding loops of HIV-1 WT, HIV-2 WT, HIVac-2 and HIVac-1 capsids.

(B) GFP and CD86 expression in DCs infected with HIV-1 WT or HIVac-1. Cells were treated or not with Raltegravir (RAL) at the time of infection. SIVmac VLPs were added to provide Vpx.

(C) Dose-response of CD86 expression as in (B) (n=5).

(D) IP-10 (CXCL10) production by DCs infected with HIV-1 WT or HIVac-1 or treated with poly(I:C) (pIC) for 48 hours, in the absence or the presence of Vpx-containing SIVmac VLPs or Raltegravir (RAL) (n=5; paired t-test on log transformed data).

Figure 6 Dendritic cells exposed to HIVac stimulate adaptive immunity

(A) Induction of costimulatory functions by HIVac-2. Expression of CD86 in DCs and proliferation of primary naïve $CD4^+$ T cells as shown by dilution of a Cell Proliferation Dye (CPD). DCs were initially infected or not with HIVac-2. AZT was added to block cDNA synthesis and SIVmac VLPs were added to increase the dose of Vpx protein.

(B) Proliferation of $CD8^+$ T cells from HIV-1-infected individuals after co-culture with autologous DCs infected super-infected by HIV-1 WT or HIVac-1 in the presence of Vpx-containing SIVmac VLPs and Raltegravir (RAL), with or with AZT (n=6, except with AZT

n=4). Cells were gated by structure, size and LIVE/DEAD. Representative plots at day 7 are shown.

(C) Quantification of $CD8^+$ T cell proliferation as in (B) measured at day 5 and day 7 (n=6, except with AZT n=4). Proliferating cells were gated by structure, size and LIVE/DEAD and as $CD4^-CD8^+CPD^{low}$.

Figure 7 cGAS is essential for dendritic cell sensing of HIV

(A) cGAS protein levels after RNAi, at day 6 after shRNA transduction in monocytes and differentiation in DCs. One representative donor is shown.

(B) Expression of CD86 and GFP in DCs transduced with a control shRNA against LacZ or a shRNA against cGAS and subsequently infected with HIV-1, HIV-2, HIVac-2 or stimulated with poly(I:C) (10 µg/ml). Of note, the shRNA transduction procedure at day 0 includes addition of Vpx-containing VLPs, which abrogates the SAMHD1 restriction for HIV-1 infection at day 4.

(C) Dose-response of CD86 in DCs transduced with shRNA as in (B) and infected with HIV-1, HIV-2, HIVac-2 (n=3).

Figure 1

A

CypA-binding loop

HIV-1 capsid HPVHAGPIAPGQMREPR
87 90

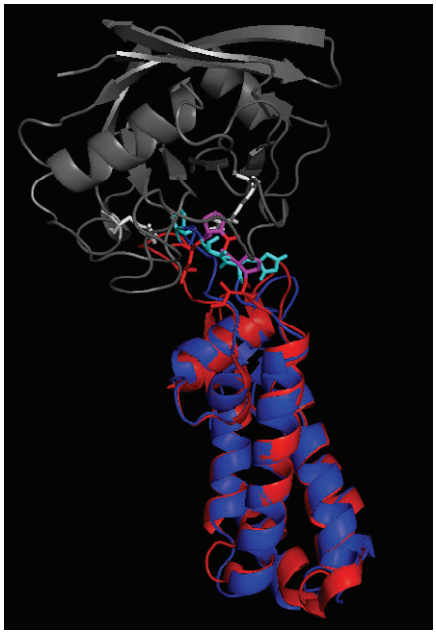
HIV-2 capsid HPIP-GPLPAGQLREPR
86 88

B

HIVac-2 HPIHAGPLPAGQLREPR
(HIV-2 P86HA)

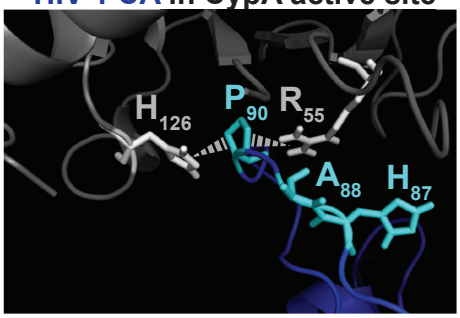
C

HIV-1 CA bound to CypA
HIV-2 CA overlay

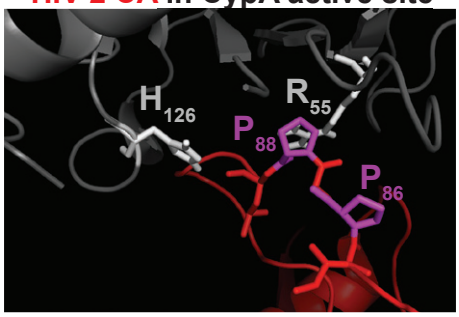


D

HIV-1 CA in CypA active site



HIV-2 CA in CypA active site



E

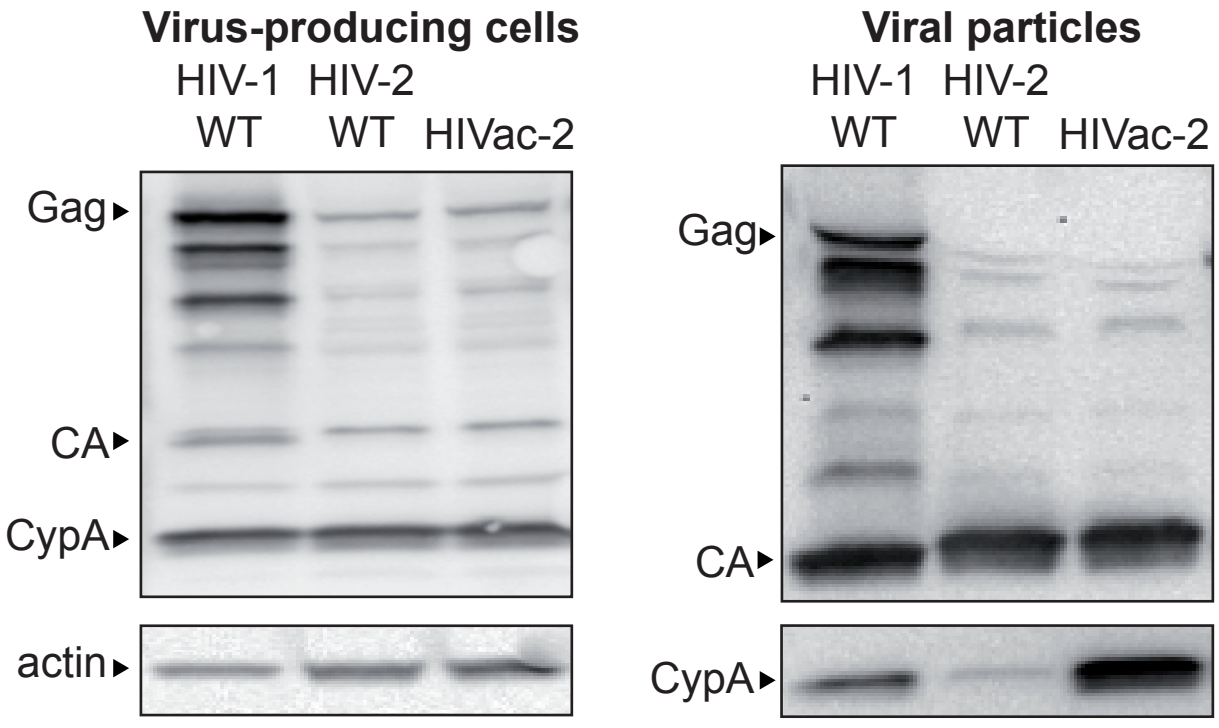


Figure 2

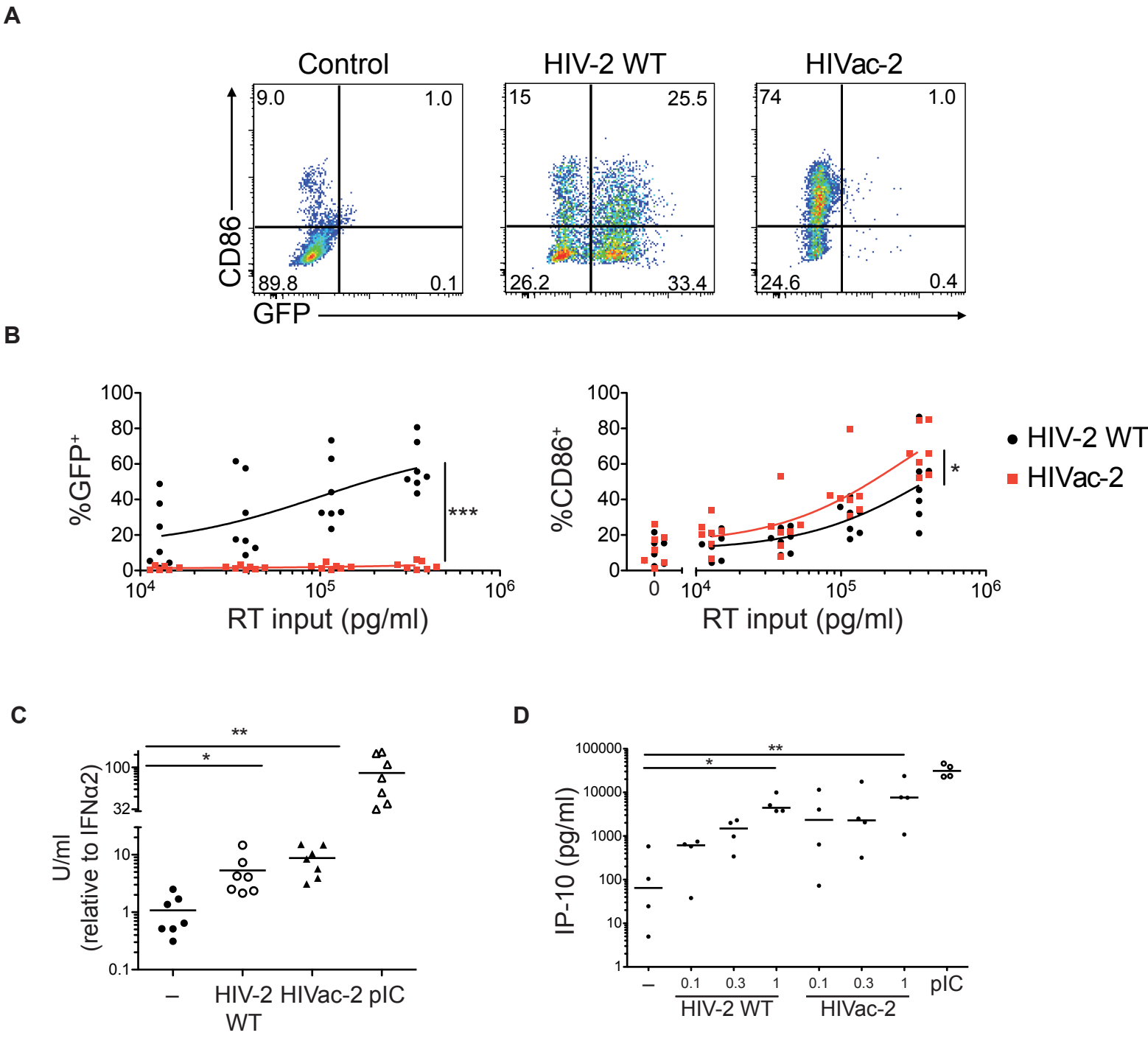

A
Control
HIV-2 WT
HIVac-2
9.0
1.0
89.8
0.1
15
25.5
26.2
33.4
74
1.0
24.6
0.4
CD86
GFP
B
%GFP+
RT input (pg/ml)
***
%CD86+
*
HIV-2 WT
HIVac-2
C
U/ml (relative to IFNα2)
**
*
–
HIV-2 WT
HIVac-2
pIC
D
IP-10 (pg/ml)
**
*
0.1
0.3
1
HIV-2 WT
HIVac-2
pIC

Figure 3

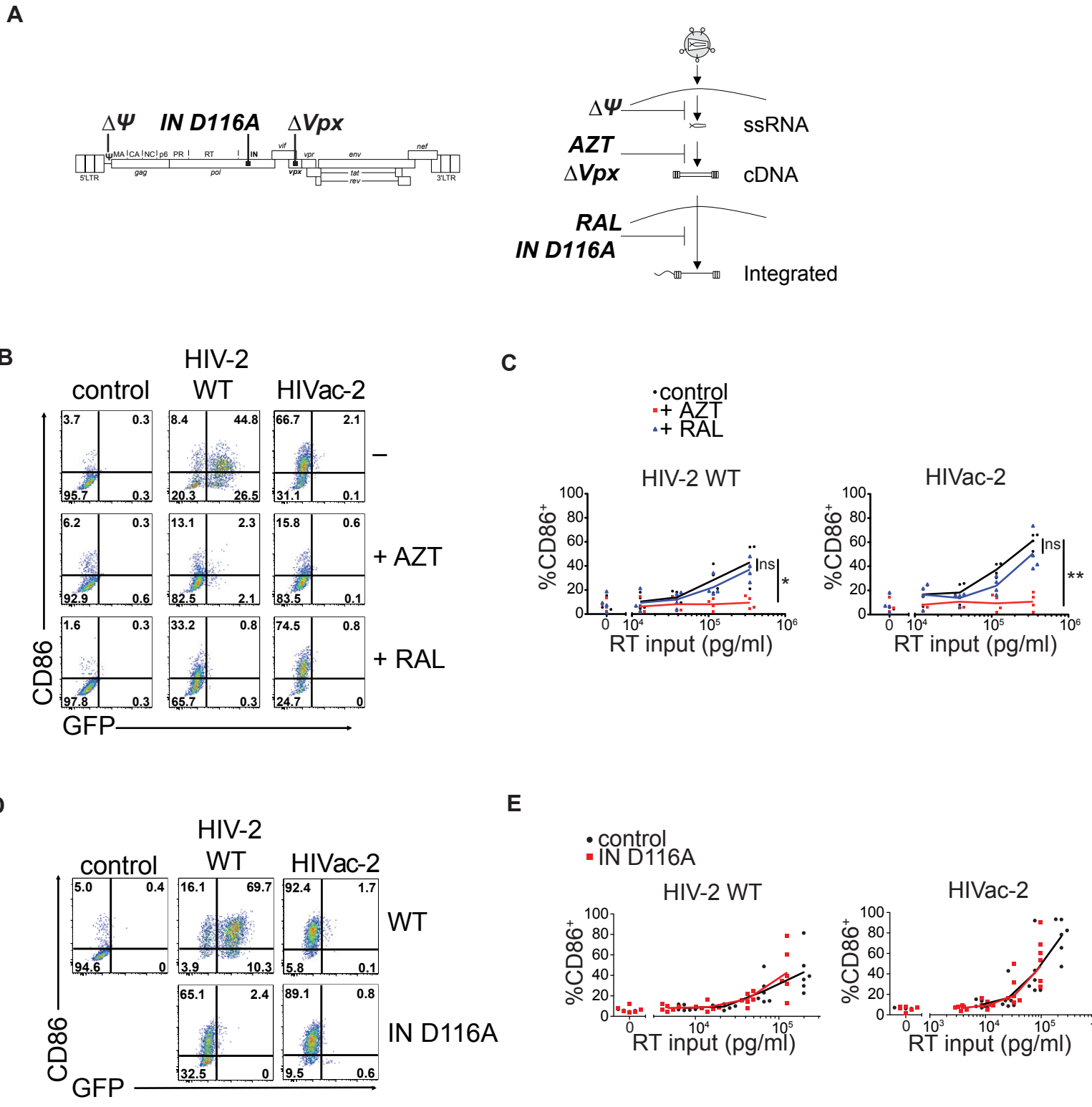
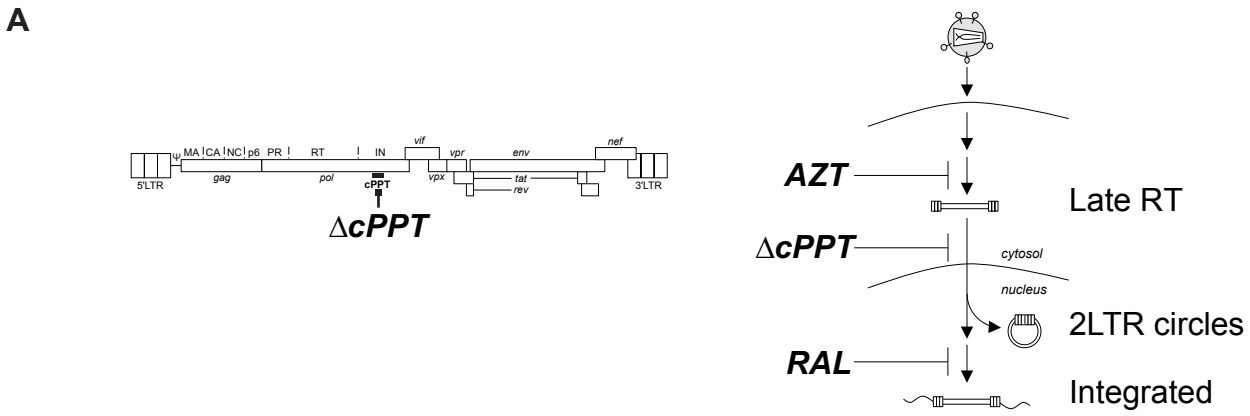
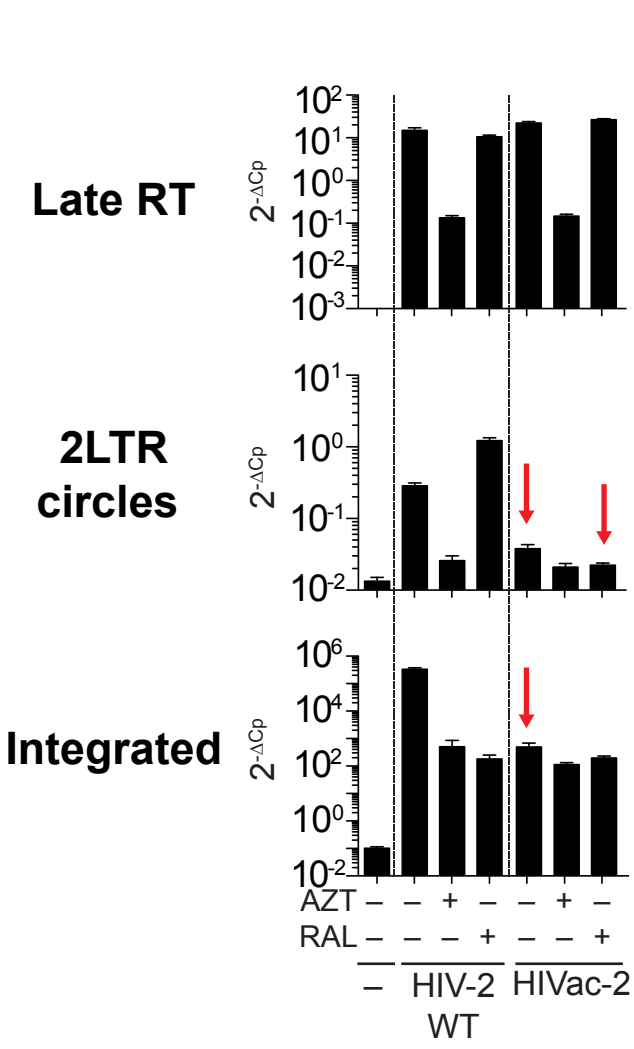
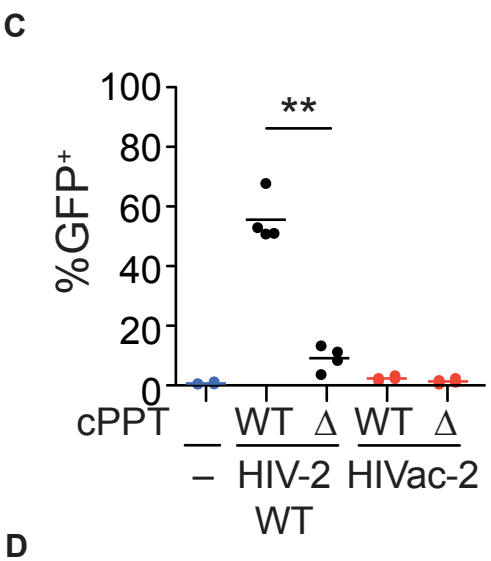

A
ΔΨ
IN D116A
ΔVpx
5'LTR
gag
pol
vif
vpr
tat
rev
vpx
env
nef
3'LTR
ΔΨ
ssRNA
AZT
ΔVpx
cDNA
RAL
IN D116A
Integrated
B
control
HIV-2 WT
HIVac-2
3.7
0.3
95.7
0.3
8.4
44.8
20.3
26.5
66.7
2.1
31.1
0.1
–
6.2
0.3
92.9
0.6
13.1
2.3
82.5
2.1
15.8
0.6
83.5
0.1
+ AZT
1.6
0.3
97.8
0.3
33.2
0.8
65.7
0.3
74.5
0.8
24.7
0
+ RAL
CD86
GFP
C
control
+ AZT
+ RAL
HIV-2 WT
HIVac-2
%CD86+
RT input (pg/ml)
ns
*
**
D
control
HIV-2 WT
HIVac-2
5.0
0.4
94.6
0
16.1
69.7
3.9
10.3
92.4
1.7
5.8
0.1
WT
65.1
2.4
32.5
0
89.1
0.8
9.5
0.6
IN D116A
CD86
GFP
E
control
IN D116A
HIV-2 WT
HIVac-2
%CD86+
RT input (pg/ml)

Figure 4


A
ΔcPPT
AZT
Late RT
ΔcPPT
cytosol
nucleus
2LTR circles
RAL
Integrated


B
Late RT
2LTR circles
Integrated
AZT
RAL
HIV-2 WT
HIVac-2


C
%GFP+
cPPT
WT
Δ
HIV-2 WT
HIVac-2

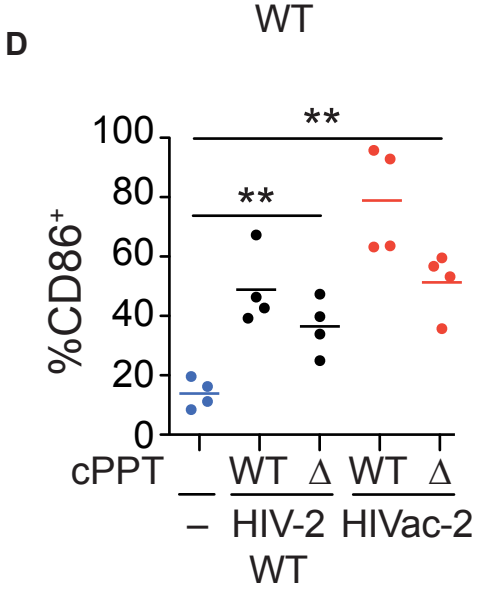

D
%CD86+
cPPT
WT
Δ
HIV-2 WT
HIVac-2

Figure 5

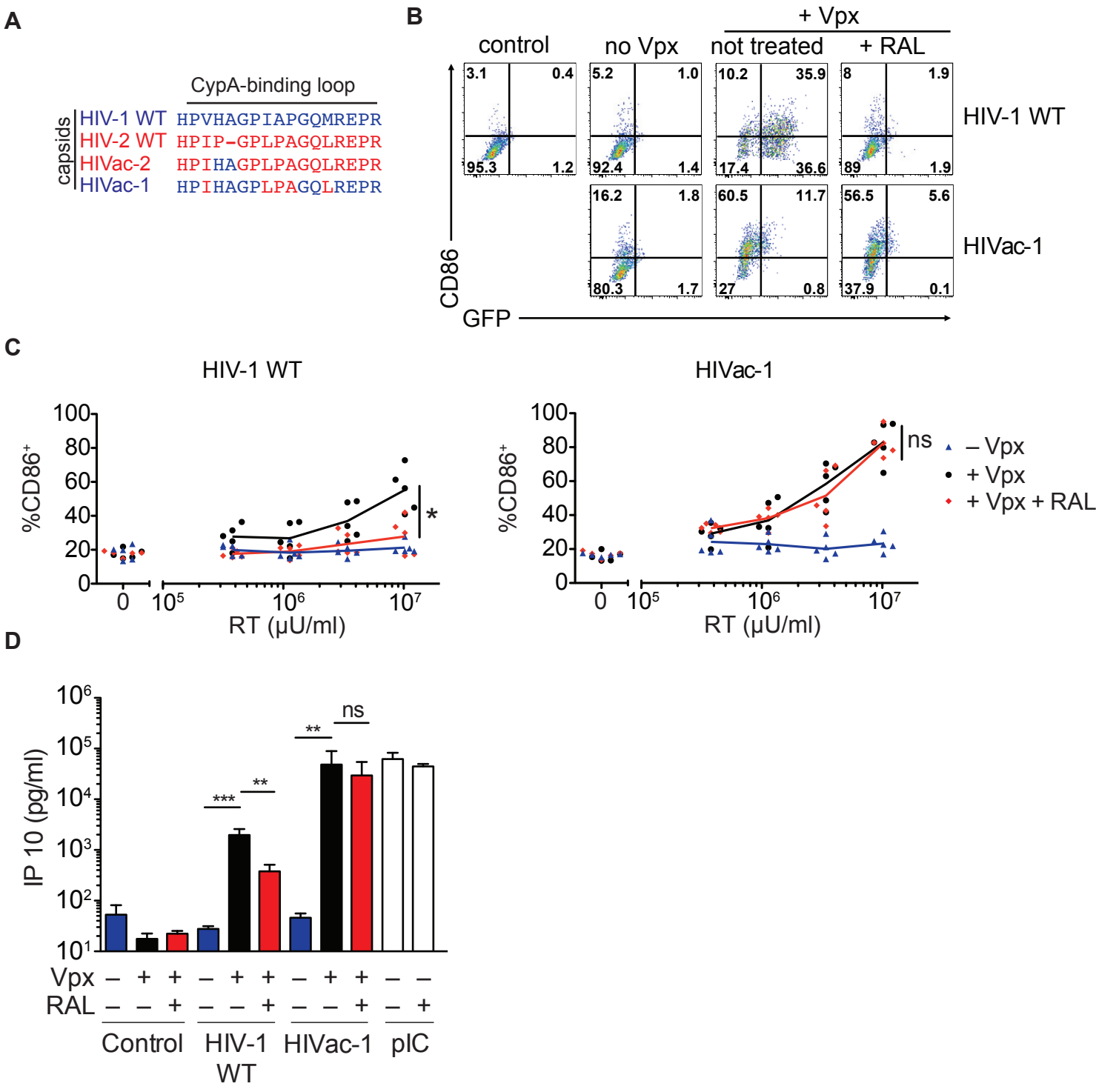

A
CypA-binding loop
capsids
HIV-1 WT HPVHAGPIAPGQMREPR
HIV-2 WT HPIP-GPLPAGQLREPR
HIVac-2 HPIHAGPLPAGQLREPR
HIVac-1 HPIHAGPLPAGQLREPR
B
+ Vpx
control
no Vpx
not treated
+ RAL
HIV-1 WT
HIVac-1
CD86
GFP
3.1
0.4
95.3
1.2
5.2
1.0
92.4
1.4
10.2
35.9
17.4
36.6
8
1.9
89
1.9
16.2
1.8
80.3
1.7
60.5
11.7
27
0.8
56.5
5.6
37.9
0.1
C
HIV-1 WT
HIVac-1
%CD86+
RT (µU/ml)
ns
*
– Vpx
+ Vpx
+ Vpx + RAL
D
IP 10 (pg/ml)
Vpx
RAL
Control
HIV-1 WT
HIVac-1
pIC
***
**
**
ns

Figure 6

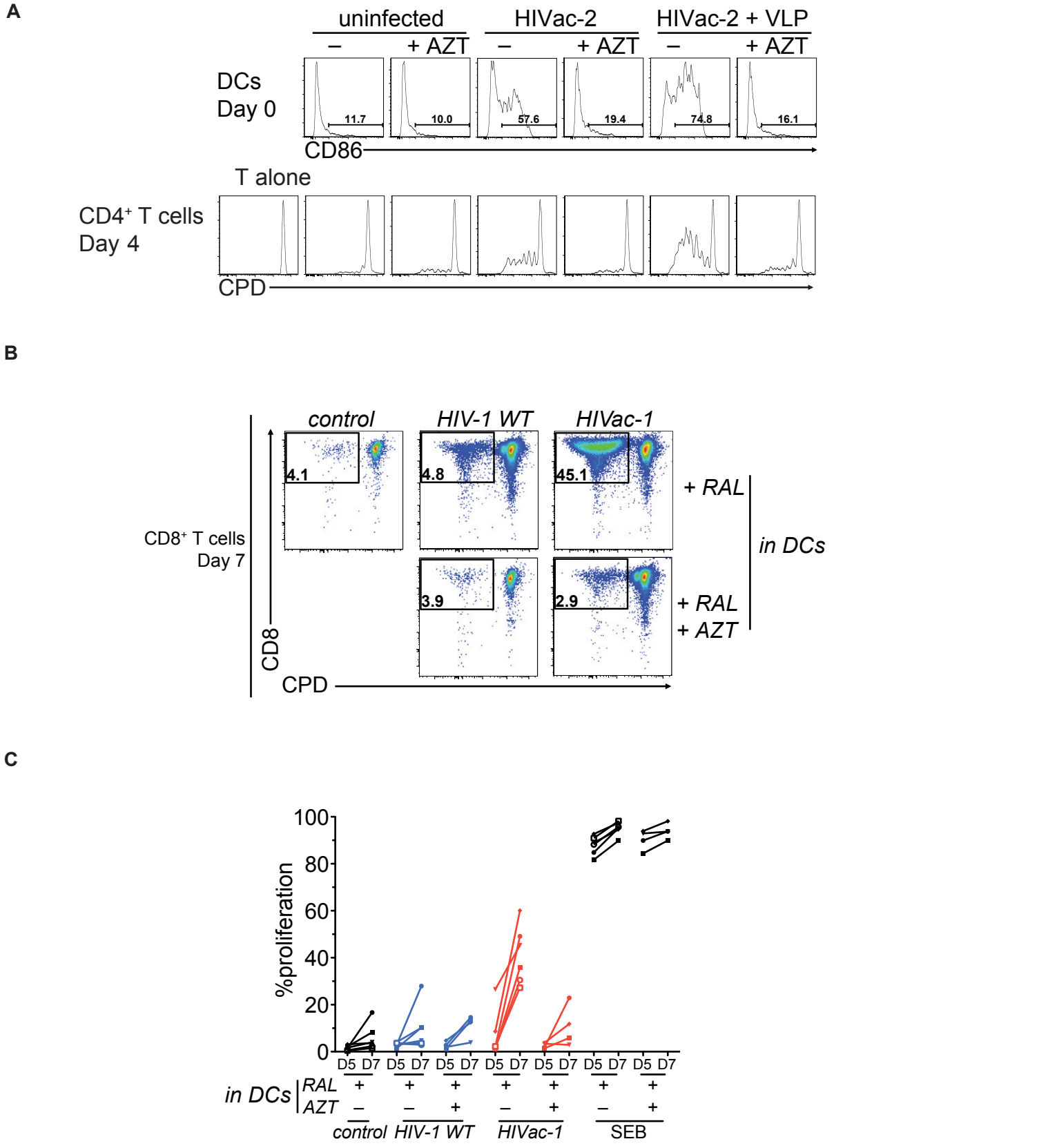

A
uninfected
HIVac-2
HIVac-2 + VLP
– + AZT – + AZT – + AZT
DCs
Day 0
11.7
10.0
57.6
19.4
74.8
16.1
CD86
T alone
CD4+ T cells
Day 4
CPD
B
control
HIV-1 WT
HIVac-1
CD8+ T cells
Day 7
4.1
4.8
45.1
+ RAL
in DCs
3.9
2.9
+ RAL
+ AZT
CD8
CPD
C
%proliferation
100
80
60
40
20
0
D5 D7 D5 D7 D5 D7 D5 D7 D5 D7 D5 D7
in DCs
RAL + + + + + + +
AZT – – + – + – +
control
HIV-1 WT
HIVac-1
SEB

Figure 7

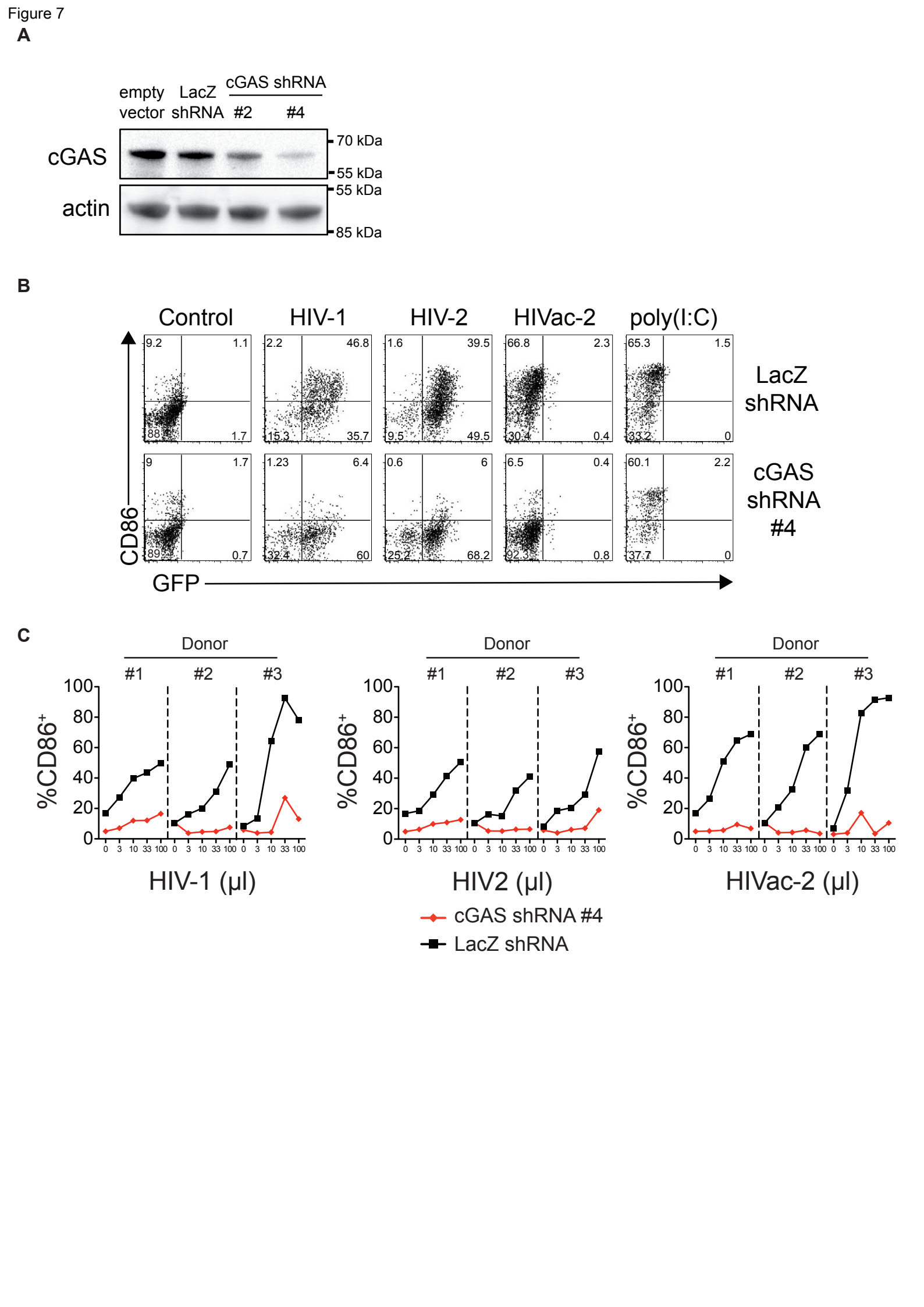

A
empty vector
LacZ shRNA
cGAS shRNA
#2
#4
cGAS
actin
70 kDa
55 kDa
55 kDa
85 kDa
B
Control
HIV-1
HIV-2
HIVac-2
poly(I:C)
LacZ shRNA
cGAS shRNA #4
CD86
GFP
9.2
1.1
88
1.7
2.2
46.8
15.3
35.7
1.6
39.5
9.5
49.5
66.8
2.3
30.4
0.4
65.3
1.5
33.2
0
9
1.7
89
0.7
1.23
6.4
32.4
60
0.6
6
25.2
68.2
6.5
0.4
92.3
0.8
60.1
2.2
37.7
0
C
Donor
#1
#2
#3
%CD86+
100
80
60
40
20
0
0 3 10 33 100
HIV-1 (μl)
HIV2 (μl)
HIVac-2 (μl)
cGAS shRNA #4
LacZ shRNA

Figure S1

Click here to download Supplemental Text and Figures: FigureS1.pdf

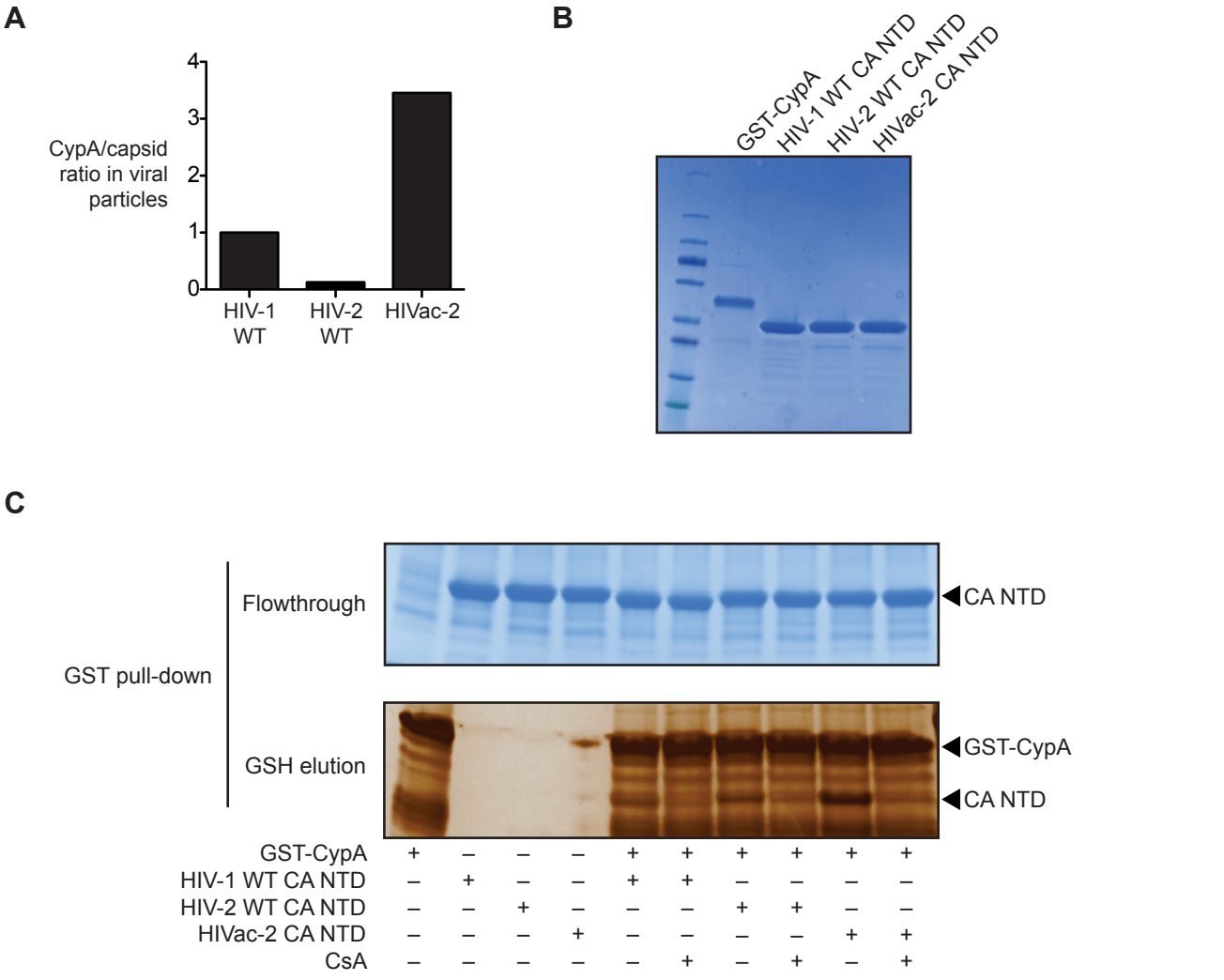


Figure S2

Click here to download Supplemental Text and Figures: FigureS2.pdf

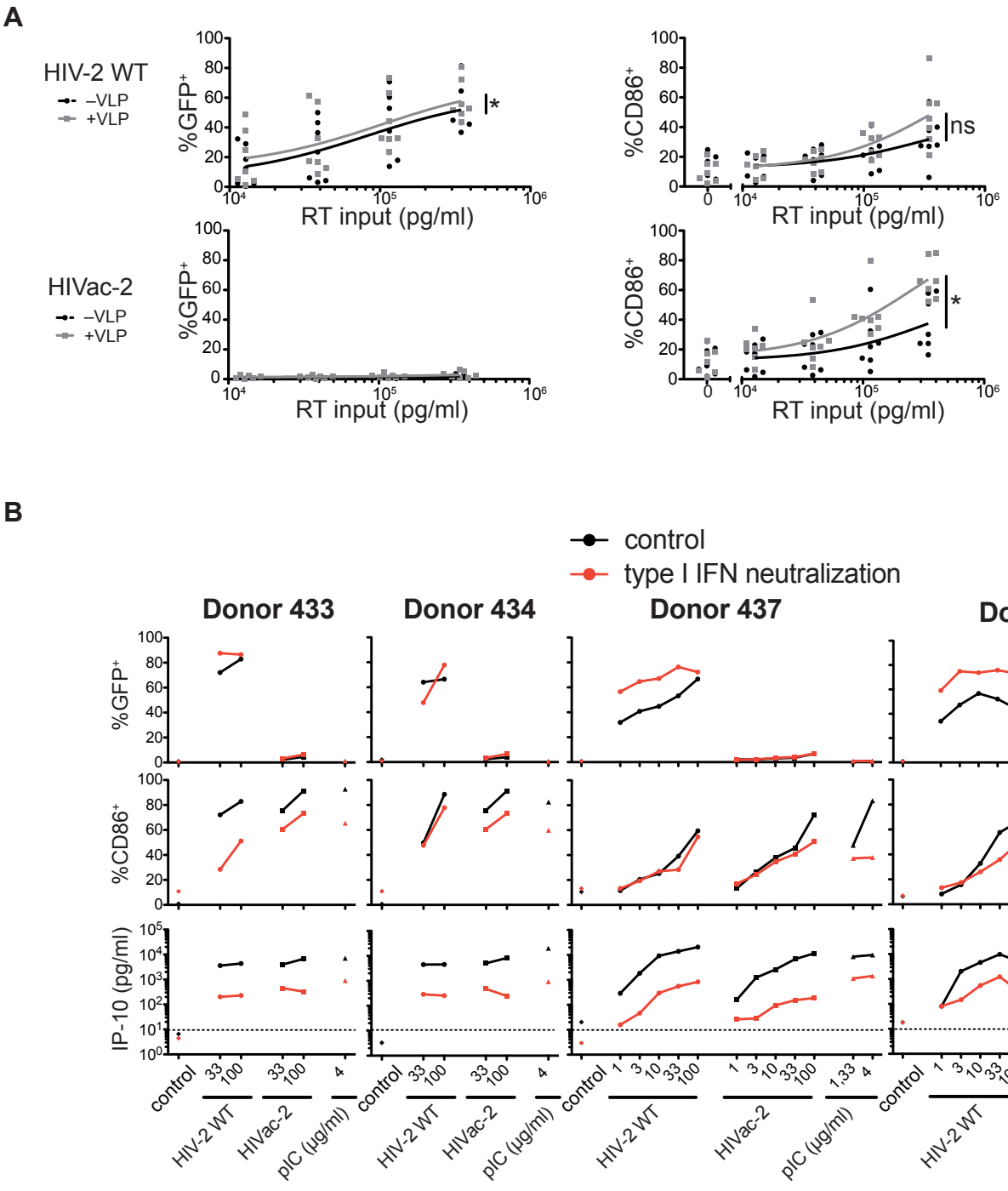


Figure S3

Click here to download Supplemental Text and Figures: FigureS3.pdf

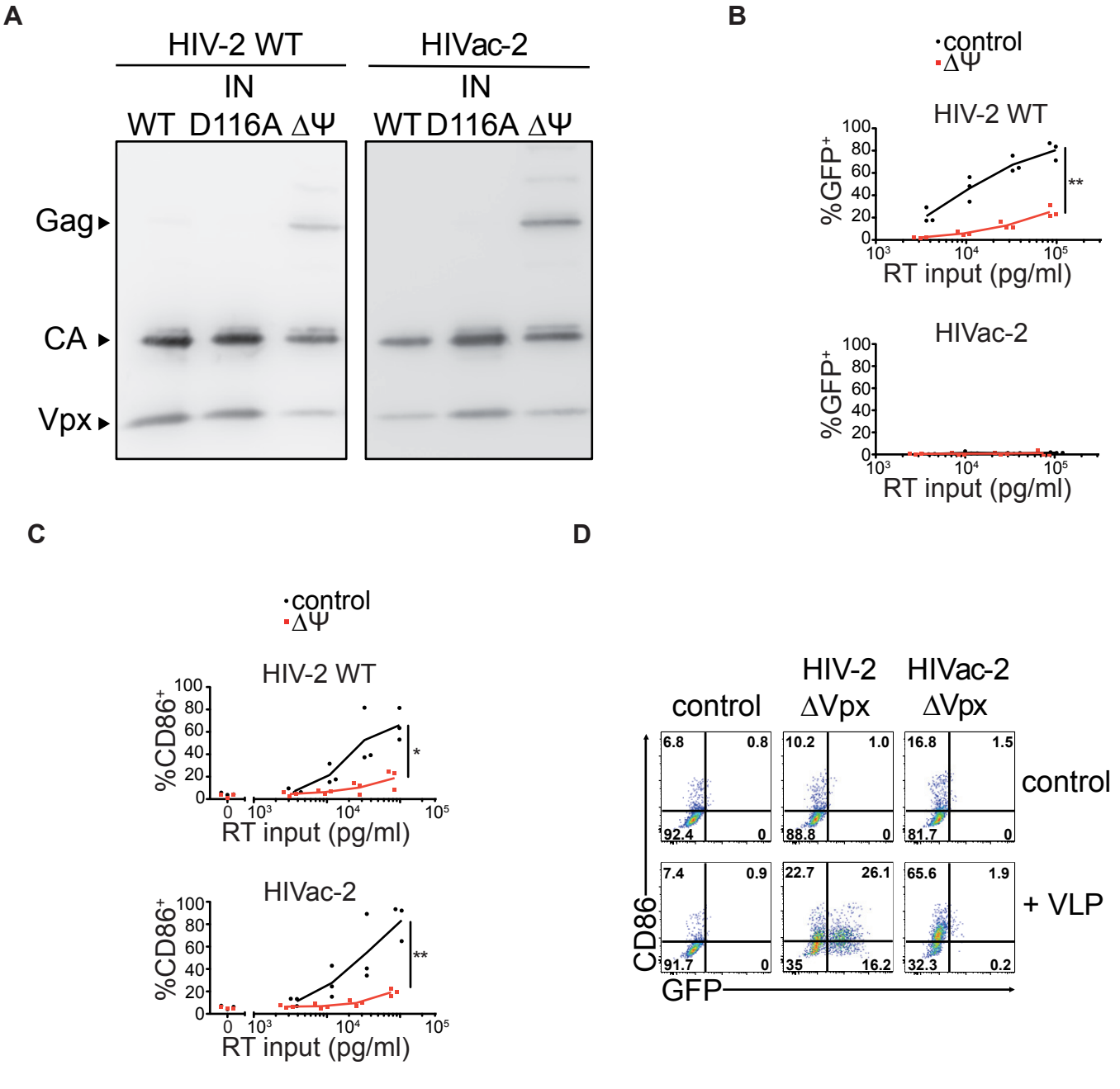


Figure S4

Click here to download Supplemental Text and Figures: FigureS4.pdf

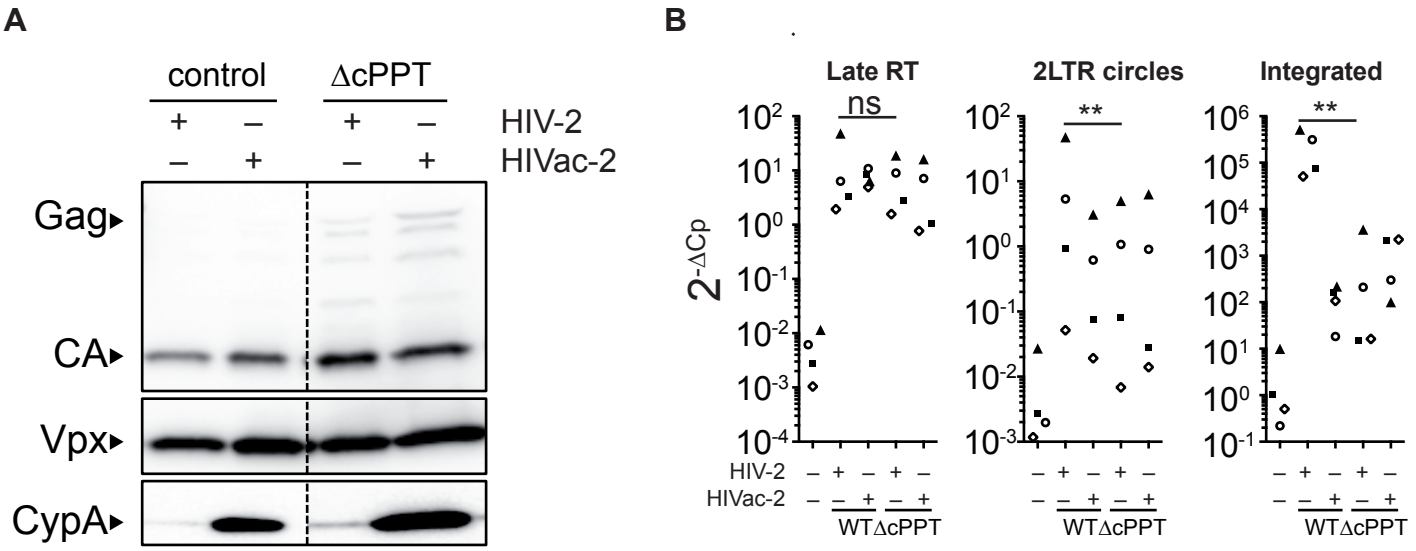


Figure S5

Click here to download Supplemental Text and Figures: FigureS5.pdf

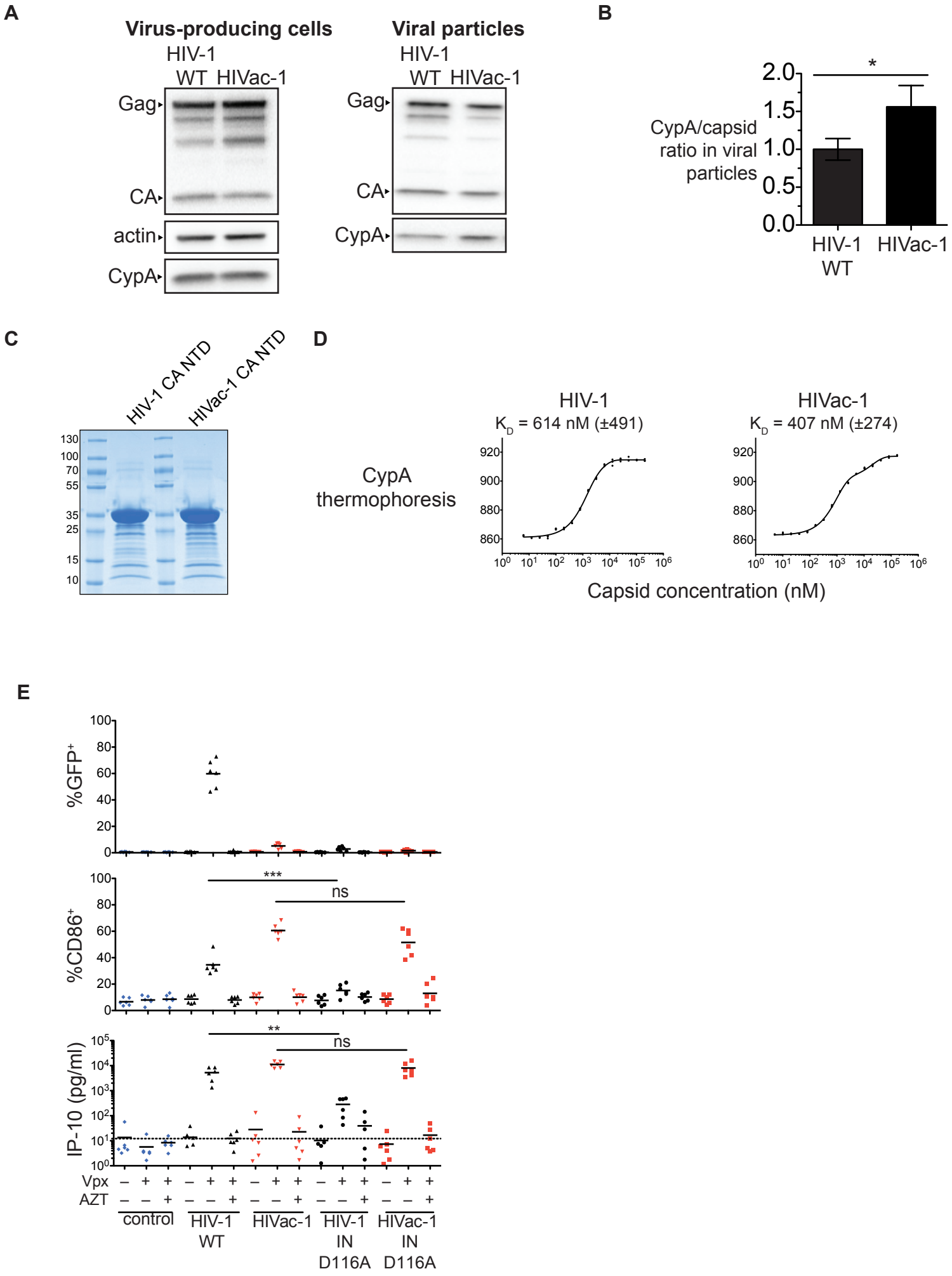


Figure S6

Click here to download Supplemental Text and Figures: FigureS6.pdf

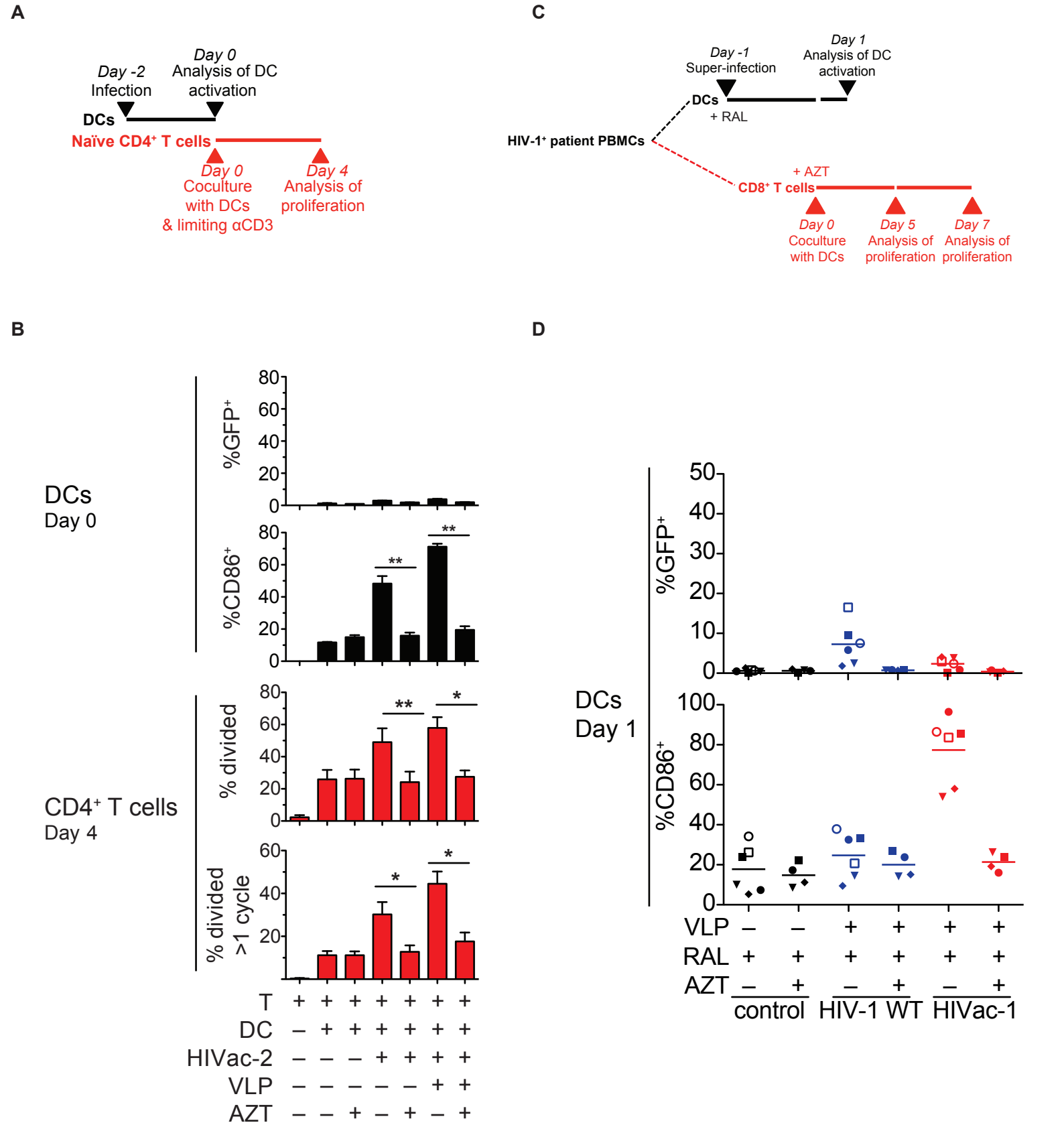


Figure S7

Click here to download Supplemental Text and Figures: FigureS7.pdf

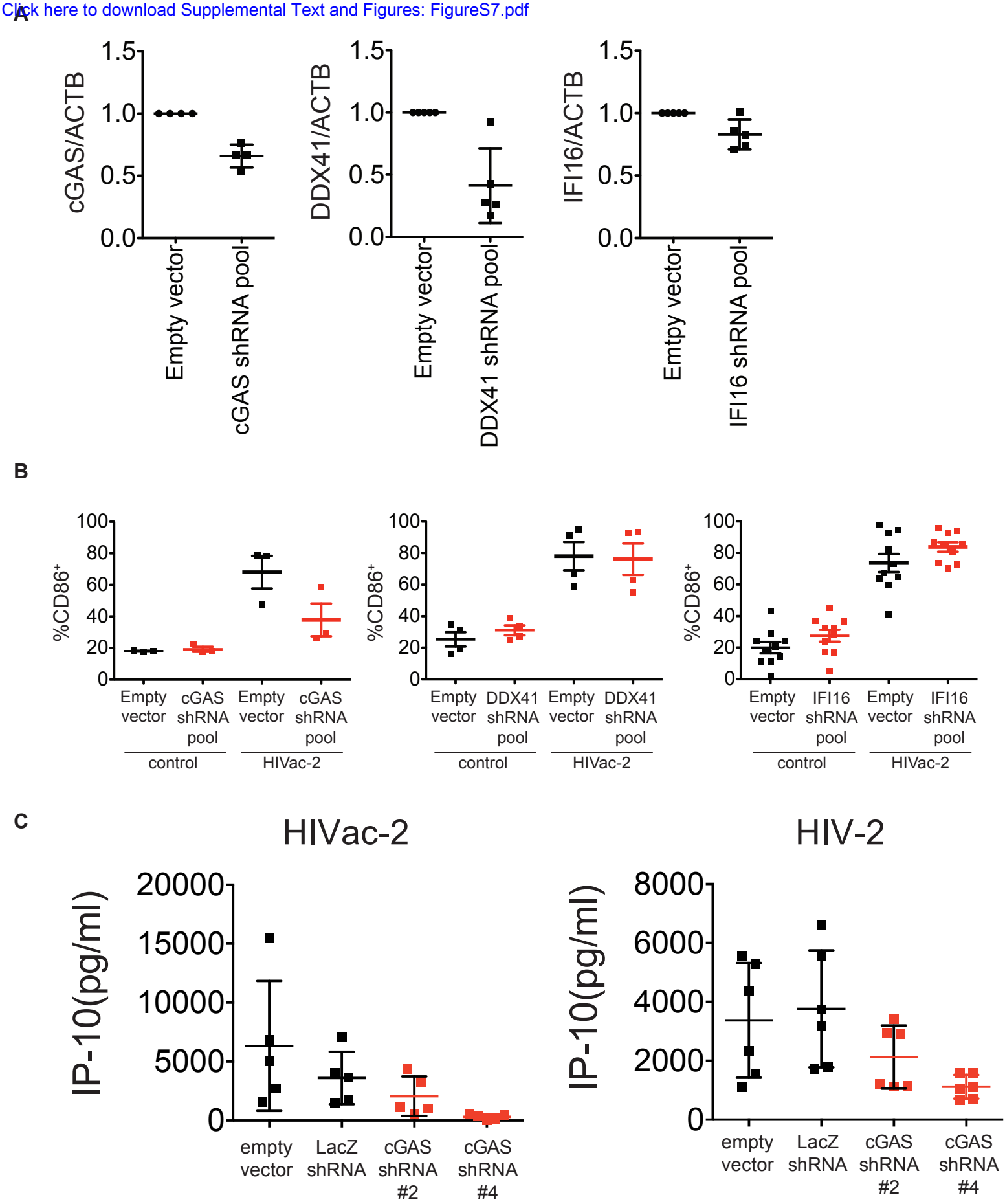
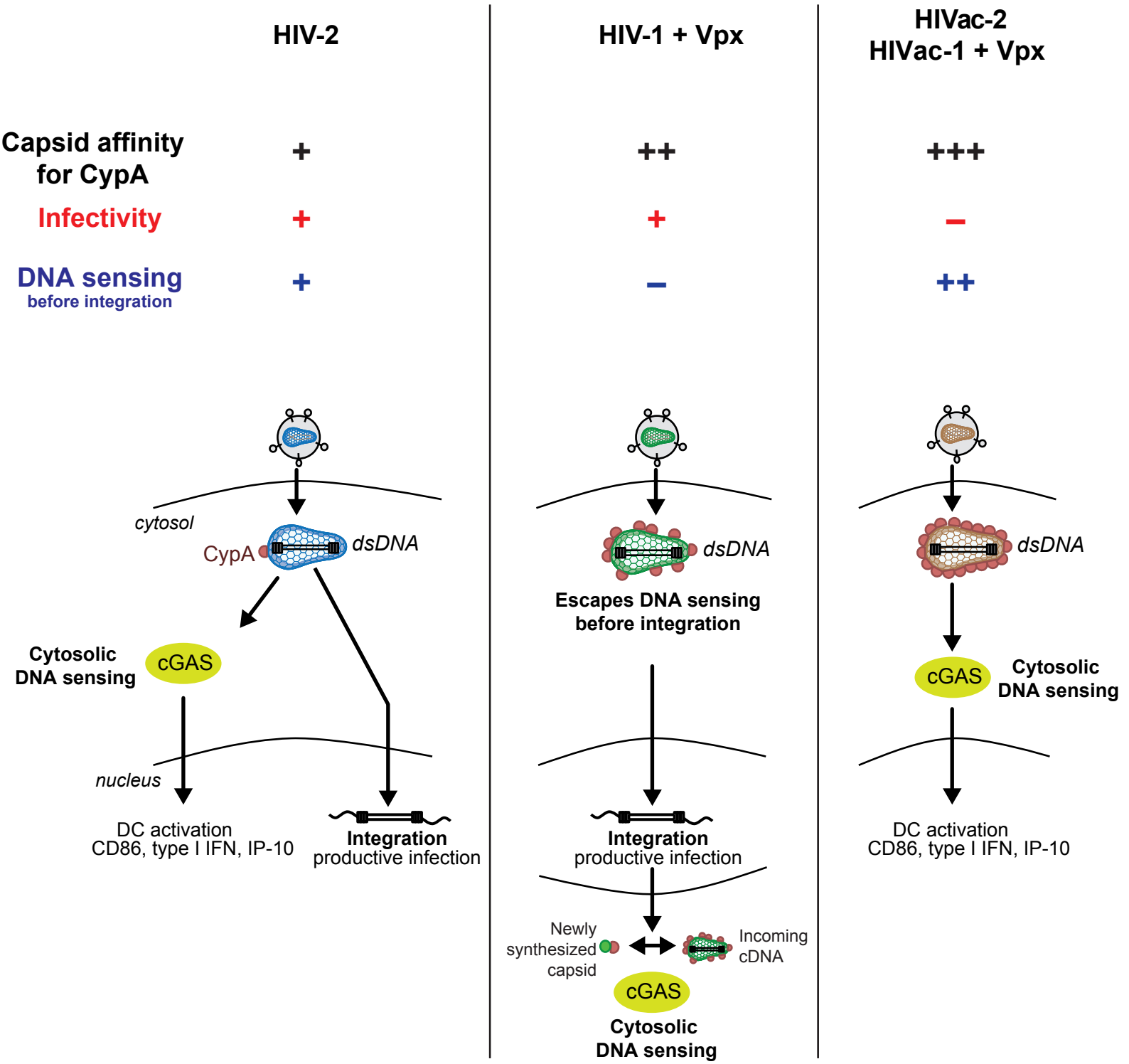


Figure S8

Click here to download Supplemental Text and Figures: FigureS8.pdf



Supplemental Material
Click here to download Supplemental Text and Figures: lahaye-supplementary-immunity.doc

Inventory of Supplemental Information

- Supplementary Figure 1 – related to Figure 1
- Supplementary Figure 2 – related to Figure 2
- Supplementary Figure 3 – related to Figure 3
- Supplementary Figure 4 – related to Figure 4
- Supplementary Figure 5 – related to Figure 5
- Supplementary Figure 6 – related to Figure 6
- Supplementary Figure 7 – related to Figure 7
- Supplementary Figure 8 – related to Discussion
- Supplementary Tables 1, 2, 3, 4, 5
- Supplementary Methods
- Supplementary References

Supplementary Figure Legends

Supplementary Figure 1

(A) Ratios of CypA over capsid in viral particles, quantified from Figure 1E. Ratios were normalized to HIV-1.

(B) Integrity and purity of the recombinant proteins. GST-CypA, HIV-1 WT or HIV-2 WT CA NTD and HIVac-2 CA NTD proteins were purified after expression in bacteria. Purified proteins were analyzed by SDS-PAGE followed by Coomassie dye staining.

(C) GST-CypA and CA NTD (HIV-1 WT, HIV-2 WT or HIVac-2) were mixed and incubated as indicated. CsA was added when noted. GST pull-down was performed to isolate the GST-CypA-associated fraction. Flow through fraction were recovered and analyzed by SDS-PAGE followed by Coomassie dye staining (Top panel). After GSH elution, the GST-CypA-associated proteins were analyzed by SDS-PAGE followed silver staining (Bottom panel).

(D) Interaction between CypA and recombinant N-terminal domains of HIV-1, HIV-2 and HIVac-2 capsids, measured by microscale thermopheresis (n=3, one representative experiment is shown).

Supplementary Figure 2

(A) GFP and CD86 expression in MDDCs 48 hours after infection with HIV-2 WT or HIVac-2. Dose-response expression of GFP and CD86 in the presence or the absence of SIVmac VLPs (n=7).

(B) GFP and CD86 expression and IP-10 production in MDDCs 48 hours after infection with HIV-2 WT or HIVac-2, with or without a type I IFN neutralization cocktail. For HIV-2 and HIVac-2, the volume of virus per well (µl) is indicated. Four individual donors are shown. The dashed line indicates the limit of sensitivity of the standard curve.

Supplementary Figure 3

(A) Detection of Gag/CA and Vpx in viral particles of HIV-2 WT or HIVac-2 that have a catalytic mutation in integrase (IN D116A) or that have a mutation in the viral RNA encapsidation signal (ΔΨ).

(B) GFP and **(C)** CD86 expression in MDDCs infected with HIV-2 WT or HIVac-2 with or without a mutation in the viral RNA encapsidation signal (n=3).

(D) GFP and CD86 expression in MDDCs infected with HIV-2 ΔVpx or HIVac-2 ΔVpx, with or without rescue with SIVmac VLPs.

Supplementary Figure 4

(A) Detection of Gag/CA, Vpx and CypA in viral particles of HIV-2 WT or HIVac-2 with or without a mutation in the cPPT (ΔcPPT).

(B) Quantification of Late RT, 2LTR and integrated viral cDNA products at 48 hours in DCs infected with HIV-2 WT or HIVac-2 that are also mutated in the cPPT (n=4, paired t-test on log-transformed data).

Supplementary Figure 5

(A) HIVac-1 particles incorporate more CypA than HIV-1 WT. Left, protein expression in virus-producing cells. HIV-1 or HIVac-1 viral proteins were analyzed by western blotting against Gag/Capsid, CypA and actin. Right, viral particles were analyzed by western blotting against Gag/Capsid and CypA.

(B) Ratios of CypA over capsid in viral particles, quantified from (A) (n=3; paired t-test before normalization). Ratios were normalized to HIV-1 WT.

(C) Integrity and purity of the recombinant HIV-1 WT CA NTD and HIVac-1 CA NTD proteins. Purified proteins were analyzed by SDS-PAGE followed by Coomassie dye staining.

(D) Interaction between CypA and recombinant HIV-1 WT CA NTD and HIVac-1 CA NTD proteins, measured by microscale thermopheresis (n=3, one representative experiment is shown, values are averages of the 3 experiments).

(E) GFP and CD86 expression and IP-10 production in DCs infected with HIV-1 WT, HIV-1 IN D116A, HIVac-1, HIVac-1 IN D116A, with of without Vpx or AZT (n=6). Cells were infected with similar amounts of particles based on RT activity. The dashed line indicates the limit of sensitivity of the standard curve.

Supplementary Figure 6

(A) Induction of costimulatory functions by HIVac-2, principle and timeline of the assay.

(B) Quantification of CD86 and GFP expression in DCs at day 0 and of the proportion of T cells that divided at day 4 (total or more than one division) (n=4).

(C) Activation of dendritic cells and stimulation of $CD8^+$ T cells from HIV-1-infected subjects, principle and timeline of the experiment.

(D) Expression of GFP and CD86 in DCs super-infected by HIV-1 WT or HIVac-1 in the presence of Vpx-containing SIVmac VLPs and Raltegravir (RAL), with or with AZT (n=6, except with AZT n=4).

Supplementary Figure 7

(A) Expression of cGAS, DDX41 and IFI16 measure by RT-qPCR at day 4 in DCs transduced with a pool of 5 shRNAs or an empty vector.

(B) CD86 expression in DCs transduced as in (A) and infected with HIVac-2.

(C) IP-10 production at day 6, in DCs transduced at day 0 with an empty vector, a control shRNA vector against LacZ or shRNA vectors #2 or #4 against cGAS and infected at day 4 with HIV-2 or HIVac-2.

Supplementary Figure 8 Model for the capsid-dependent cDNA sensing of HIV-2 or HIV-1 + Vpx by dendritic cells.

Supplementary Tables

Supplementary Table 1 Mutagenized sequences used in the study.

Backbone	**Mutation**	**Original DNA sequence**	**Mutagenized sequence**
HIV-1	V86I-IAP91LPA-M96L (HIVac-1)	CAT CCA **GTG** CAT GCA GGG CCT **ATT GCA CCA** GGC CAG ATG	CAT CCA **ATC** CAT GCA GGG CCT **CTT CCA GCA** GGC CAG CTG
HIV-2	P86HA (HIVac-2)	CAT CCA ATA **CCA** GGC CCC TTA	CAT CCA ATA **CAT GCA** GGC CCC TTA
HIV-2	D116A	TTG CAT ACA **GAT** AAT GGT GCC	TTG CAT ACA **GCT** AAT GGT GCC
HIV-2	ΔΨ	GCG GCA GGA **ACA AAC CAC GAC GGA GTG CTC CTA GAA AG**G CGC GGG CCG AGG TAC CAA AGG CAG CGT GTG GAG CGG GAG GAG AAG AGG CCT CCG GGT GAA GGT AAG TAC CTA CA**C CAA AAA CTG TAG CCG AAA GGG CTT GCT ATC CTA CCT TTA GAC AGG TAG AAG ATT GTG GG**A GAT GGG	GCG GCA GGA::GCG CGG GCC GAG GTA CCA AAG GCA GCG TGT GGA GCG GGA GGA GAA GAG GCC TCC GGG TGA AGG TAA GTA CCT A::GA TGG GC
HIV-2	ΔVpx	TGC AAC AAA **ATG** ACA GAC CC	TGC AAC AAA **ACG** ACA GAC CC
HIV-2	ΔcPPT	ATG GCA GTT CAT TGC ATG **AAT TTT AAA AGA AGG GGG GGA** ATA GGG	ATG GCA GTT CAT TGC ATG AAc **TTC AAG CGC CGC GGT GGT** ATA GGG

Supplementary Table 2 shRNA used in the study.

Gene	*shRNA identifier*	*TRC identifier*	*Target sequence*
DDX41	#1	TRCN0000001267	GCCACTACCTTCATCAACAAA
DDX41	#2	TRCN0000001268	GAGGAGATTGAGAACTATGTA
DDX41	#3	TRCN0000001269	CCATCCAGCACGTCATCAATT
DDX41	#4	TRCN0000001270	CGCCACTACCTTCATCAACAA
DDX41	#5	TRCN0000001271	AGACCAGGAGGAACGGACTAA
IFI16	#1	TRCN0000019079	GCAAATTATGTTTGCCGCAAT
IFI16	#2	TRCN0000019080	GACAGGACAATGTCACAATAT
IFI16	#3	TRCN0000019081	GTCAGGTAACTCCCAGAAGAA
IFI16	#4	TRCN0000019082	CCAAAGAAGATCATTGCCATA
IFI16	#5	TRCN0000019083	CTGATTCAAGTATGGAAACTT
MB21D1	#1	TRCN0000148226	GAAGAGAAATGTTGCAGGAAA
MB21D1	#2	TRCN0000148605	CAGCTTCTAAGATGCTGTCAA
MB21D1	#3	TRCN0000149811	GCTTTGATAACTGCGTGACAT
MB21D1	#4	TRCN0000149984	CAACTACGACTAAAGCCATTT
MB21D1	#5	TRCN0000150010	CCTGCTGTAACACTTCTTATT

Supplementary Table 3 Antibodies used in the study.

Antigen	*Source*	*Clone or name*
CD86	eBioscience	IT2.2
CD3	eBioscience	OKT3
CD14	eBioscience	61D3
CD8ß	Coulter	2ST8.5H7
CD8	BD	RPA-T8
CD4	Invitrogen	S3.5
CD4	eBioscience	RPA-T4
CD45RO	BD	UCHL1

CD27	BD	M-T271
Gag/capsid	The following reagent was obtained through the AIDS Research and Reference Reagent Program, Division of AIDS, NIAID, NIH: HIV-1 p24 Hybridoma (183-H12-5C) from Dr. Bruce Chesebro.	183-H12-5C
Vpx	The following reagent was obtained through the AIDS Research and Reference Reagent Program, Division of AIDS, NIAID, NIH: HIV-2 Vpx Hybridoma (6D2.6) from Dr. John C. Kappes.	6D2.6
Actin	Millipore	C4
CypA	Wes Sundquist lab	UT96
IFNα	eBioscience	EBI-1
IFNß	eBioscience	A1
IFNß	Millipore	A1
IFNAR2	Millipore	MMHAR-2
cGAS	SIGMA	HPA031700

Supplementary Table 4 Characteristics of the HIV-1 patients. Values are indicates as mean and range.

	Characteristics
Number	6
Age (year)	40.6 (21-56)
Male/Female	4/2
Infection duration (years)	14 (4-23)
Treatment duration (years)	6,9 (0.5-20.5)
CD4 nadir (cells/mm^3)	218 (5-350)
VL baseline, copies/mL [1]	120.000 (2640-20600)
CD4 (cells/mm^3) [2]	547 (274 – 950)
CD8 (cells/mm^3) [2]	901 (409-1510)
CD4/CD8 ratio [2]	0.75 (0.19 -1.12)

[1] at treatment initiation

[2] at the entry in the study

Supplementary Table 5 Real-time quantitative PCR primers used in the study

Primer name	*Sequence*
DDX41qPCR-F	GCGACAGATGTCTAGGCTGA
DDX41qPCR-R	CATGTCCGTGAAAGAGCAGA
ifi16-2068-f	TTGTGGCTGATGTGAATGCTGACCG

ifi16-2414-r	CCTGGTCTTGATGACCTTGATGTGAC
cGASqPCR-F	AAGGATAGCCGCCATGTTTC
cGASqPCR-R	TGGCTTTCAGCAAAAGTTGG
bactin737f	GGACTTCGAGCAAGAGATGG
bactin970r	AGCACTGTGTTGGCGTACAG

Supplementary Methods

Recombinant protein expression and purification

Protein-expression vectors were transformed in *E. Coli* BL21 Star (DE3) (Invitrogen). Bacteria were plated on Ampicillin 0.1 µg/ml and Chloramphenicol 34 µg/ml. Single colonies were expanded in 2YT media with Ampicillin and Chloramphenicol 34 µg/ml at 37°C overnight. Pre-cultures were diluted to OD_{600} 0.05 and expanded up to OD_{600} 0.5. Protein expression was induced with IPTG 1 mM for 4 h at 30°C. Cells were washed in PBS and frozen. Bacteria were lysed for 1 h at 4°C on a rotating wheel in PBS supplemented with 150 mM NaCl, 1 mg/ml lysozyme (Sigma), 10 mM $MgCl_2$, 100 µg/ml DNAse I (Roche), 0,5% Triton X-100, 15 mM imidazol and protease inhibitors (EDTA-free Complete cocktail, Roche). Lysates were clarified by centrifugation for 30 min at 75600 g and 4°C. His-tagged proteins were bound to Protino Ni-NTA agarose gel (Macherey-Nagel) for 1 h at 4°C on a rotating wheel. Beads were centrifuged for 10 min at 470 g and 4°C, washed two times in PBS supplemented with 350 mM NaCl and 15 mM imidazole, and 1 time in 50 mM Tris-HCl pH 8. Beads were packed in columns (Machery-Nagel), and proteins were eluted in 50 mM Tris-HCl pH 8 with 250 mM imidazol. Proteins were quantified using a Bradford assay (Bio-Rad) and BSA standards (Pierce). His-ZZ-Capsid NTD proteins were stored at -20°C in elution buffer, and His-GST-CypA was stored at -20°C in elution buffer supplemented with 10% glycerol. Integrity and purity of each protein was analyzed by SDS-PAGE followed by Coomassie dye staining (LabSafe GEL Blue).

CA-CypA protein interaction analysis

Protein-protein interactions were performed with MagneGST Glutathione beads (Promega). All the steps were performed at 4°C on ice. The beads were washed two times with Binding/Wash buffer (4.2 mM Na_2HPO_4, 2 mM K_2HPO_4, 140 mM NaCl, 10 mM KCl) and

one time with Binding/Wash buffer supplemented with filtered 0.1% BSA (Euromedex). Beads were then saturated in Binding/Wash buffer supplemented with 0.1% BSA and incubated on a rotating wheel for one hour. Protein interaction reactions were performed with 50 µg His-GST-CypA and 200 µg His-ZZ-Capsid NTD incubated for one hour on a rotating wheel. 10 µM CsA (Sigma) was added when noted. Proteins were next incubated with the beads for one hour on a wheel. Flow through fractions were isolated. Beads were washed 3 times in Binding/Wash buffer, with or without CsA. After the last wash, beads were incubated 15 min with gentle mixing in elution buffer (50 mM reduced glutathione (GSH) pH 7.0-8.0 (Sigma) in PBS pH 7.4 (Gibco)). Flowthrough fractions and eluates were analyzed by SDS-PAGE followed respectively by Coomassie staining and silver stain staining (BioRad Dodeca).

Microscale Thermopheresis analysis

For MST, fresh affinity-purified recombinant His-ZZ-CA-NTD and His-CypA were further purified by fast protein liquid chromatography on Äkta systems (GE Healthcare Life Sciences). A Superdex 75 10/30 column balanced in PBS was used for the separation. All runs were performed at 10°C. Fraction were checked by Coomassis SDS-PAGE, pooled and concentrated using Amicon Ultra-4 10K filter units. His-CypA was further labeled with the Monolith NT Protein Labeling Kit BLUE according to the recommendations of the manufacturer (NanoTemper Technologies). Protein concentrations and protein–dye ratios were determined on a NanoDrop 2000 (Thermo Scientific) using extinction coefficient predicteds by ProtParam (Artimo et al., 2012). Protein-protein interactions were analyzed by MST on a Monolith NT.115 (NanoTemper technologies) using standard capillaries. His-ZZ-Capsids were 2-fold diluted sixteen times in PBS-Tween 0,05% and a one-to-one volume of His-CypA was added to a constant concentration of 500mM final. All measures were

performed at 20°C, Laser power at 10% and LED power adjusted between 20 and 50% depending on the labeling intensity. All measures were performed in two or three locations per capillary, and measures were repeated independently three times. Kd values were calculated in the NTAnalysis software (NanoTemper technologies).

Gene expression quantification

Four days after lentiviral vector transduction, total RNA was extracted from 250,000 MDDCs using Nucleospin RNA II kit (Macherey-Nagel). cDNA was synthesized with random hexamer from 0.1µg total RNA using SuperScript III Reverse Transcriptase (Invitrogen). Real-time qPCR was performed using SYBR Green I Master (Roche). Expression level of mRNA was calculated with the standard curve method. The primer sequences are listed in **Table S5**.

Western Blotting

0.2 to 2 millions cells were lysed in 80 µL of Lysis buffer (50 mM Tris Hcl pH8, 120 mM NaCl, 4 mM EDTA, 1% NP40 and 1x EDTA-free protease inhibitors cocktail (Roche)). Lysates were cleared by centrifugation at 5500 g for 7 minutes at 4°C. Virus supernatants were filtered at 0.45 µm, centrifugated at 16000 g for 1 h 30 min at 4°C. Virus pellets were lysed in 15 µl of Lysis buffer. Cellular and viral protein lysates were resolved on 4%-20% Biorad precast SDS-PAGE gels and transferred on nitrocellulose membrane. Proteins were blotted with antibodies as follow: mouse anti-Gag/capsid; mouse anti-Vpx; mouse anti-actin; rabbit anti-CypA. ECL signal was recorded on the ChemiDoc XRS Biorad Imager. Data was analyzed and quantified with the Image Lab software (Biorad).

Statistics

Statistical analyses were performed in Prism (GraphPad). The paired t-test was used, unless indicated otherwise in figure legends. In figures, * $p<0.05$, ** $p<0.01$, *** $p<0.001$, ns=not significant.

Supplementary References

Artimo, P., Jonnalagedda, M., Arnold, K., Baratin, D., Csardi, G., de Castro, E., Duvaud, S., Flegel, V., Fortier, A., Gasteiger, E., *et al.* (2012). ExPASy: SIB bioinformatics resource portal. Nucleic Acids Res *40*, W597-603.